Mechanism based Modeling of Corrosion Product Behavior in the PWR Primary Coolant System with a Thermodynamic Solubility Surrogate model

Dongmin Kim
Nuclear Fuel Cycle & Non-proliferation Lab,
Seoul National University
professor14@snu.ac.kr

June. 19th, 2026

Necessity of a CRUD Source-Term model

- **Goal: ensure core stability and operational reliability under high power, long cycle operation[1]**

원자로시설 등의 기술기준에 관한 규칙

- 제22조(원자로냉각계통 등) ① 원자로냉각계통과 그와 관련된 보조계통·제어계통·보호계통은 정상운전 및 예상운전과도 동안 원자로냉각재압력경계 설계조건을 초과하지 아니하도록 충분한 여유도를 가져야 한다.
- Korean nuclear safety rule Article 22 (① RCS pressure margin)

원자로시설 등의 기술기준에 관한 규칙

- 제22조(원자로냉각계통 등) ③ 원자로냉각계통은 냉각재중의 방사성물질의 농도 및 수질조건을 규정된 운전제한치 이하로 유지하고 처리할 수 있도록 하여야 한다.
- Korean nuclear safety rule Article 22 (① RCS pressure margin (③ radioactivity/water-quality limits)

Necessity of a CRUD Source-Term model

- **Goal: ensure core stability and operational reliability under high power, long cycle operation**
  - CRUD lowers core safety and operational reliability — CIPS, CILC, and worker dose[2]
  - Corrosion products released from steam generators and piping in the primary circuit grow into CRUD

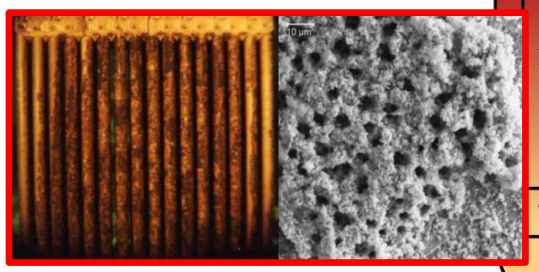

Fig Real image of CRUD deposits on the upper span of fuel[1]

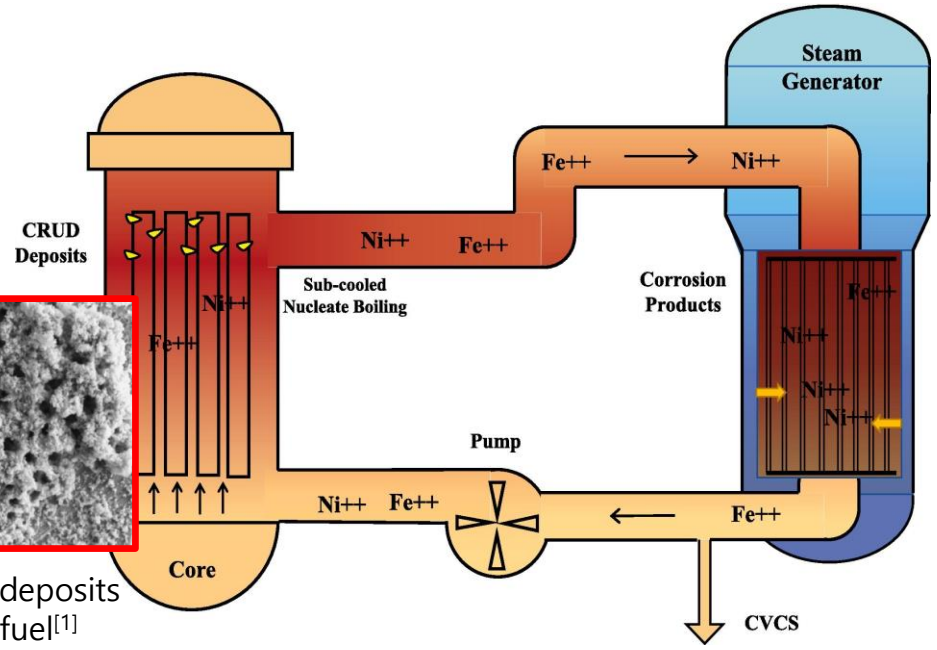

Fig Schematic of corrosion product transport and crud deposition in primary circuit of PWR[2]

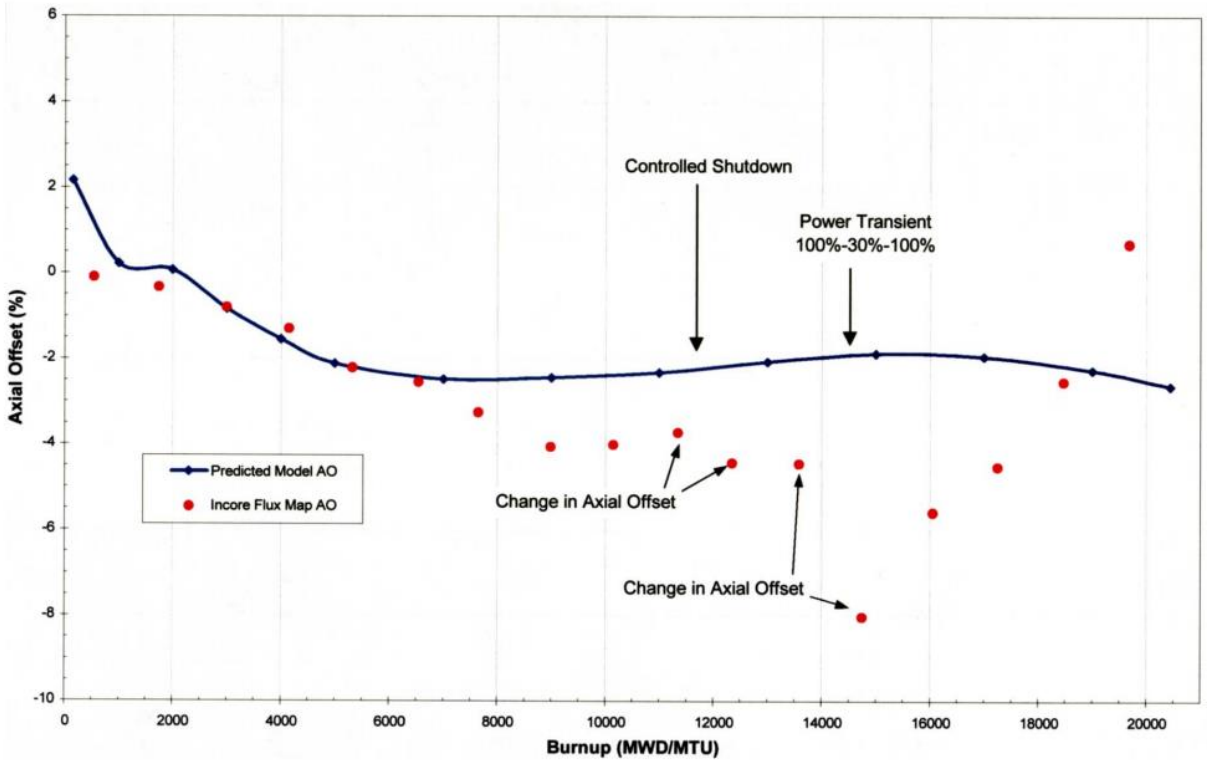

Fig Axial Offset Behavior Following Power Maneuver and Controlled Shutdown Mid-Cycle[1]

Necessity of a CRUD Source-Term model

- **Goal: ensure core stability and operational reliability under high power, long cycle operation**
  - CRUD is porous in PWRs and dense in BWRs
  - It thickens on the upper fuel; boron is trapped (hideout) and absorbs neutrons
    - → Power shifts toward the lower core — axial offset anomaly (AOA)[3]

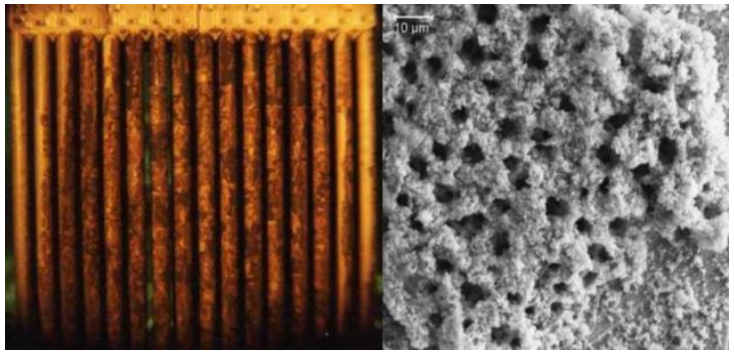

Fig Real image of CRUD deposits on the upper span of fuel[1]

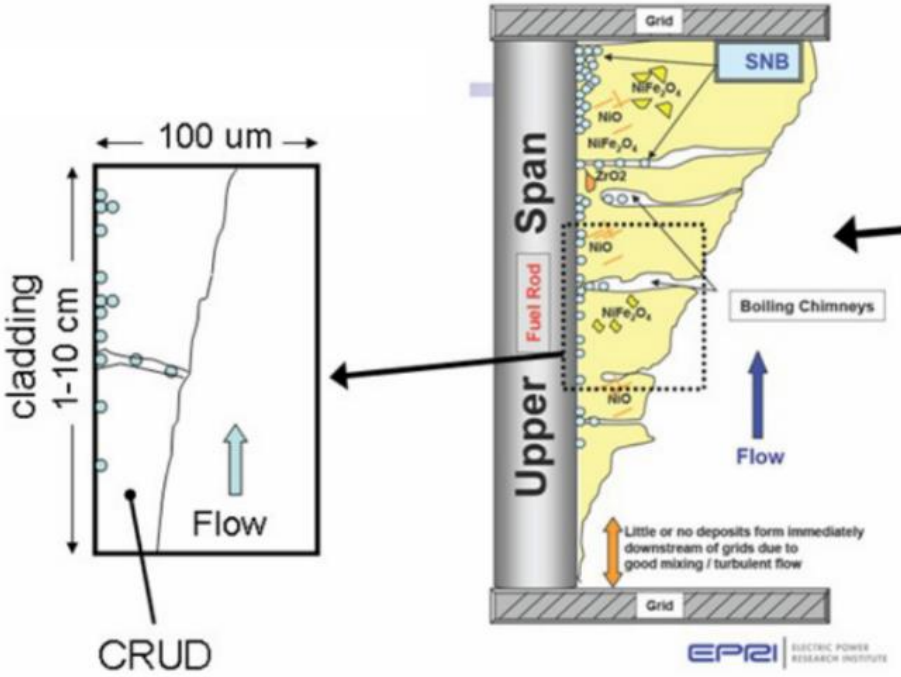

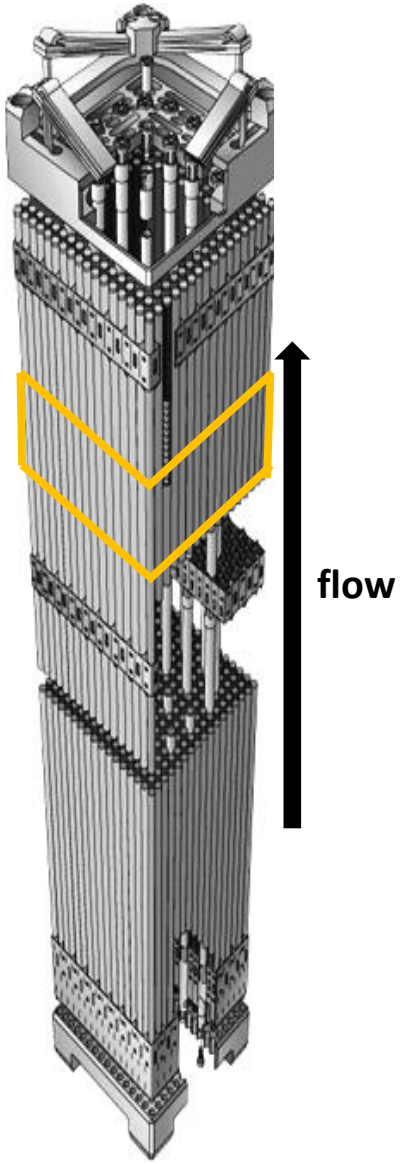

Necessity of a CRUD Source-Term model

- **Goal: ensure core stability and operational reliability under high power, long cycle operation**
  - CRUD properties[4,5,6]
    - $NiFe_2O_4$, NiO, ZrO_2, Fe_3O_4, Ni^a, $LiBO_2$, $Li_2B_4O_7$, Ni_2FeBO_5
    - Solid density = 4 ~ 6 g/cm^3
  - CRUD effects
    - CIPS: CRUD-induced Power Shift (CRUD growth & boron hideout)
    - CILC: CRUD-induced localized corrosion
  - Economic loss from AOA[7]
    - Power derating for shutdown-margin (tens of millions USD, Callaway)
    - Extra fuel assemblies for high-power operation (~1 M USD, Callaway)

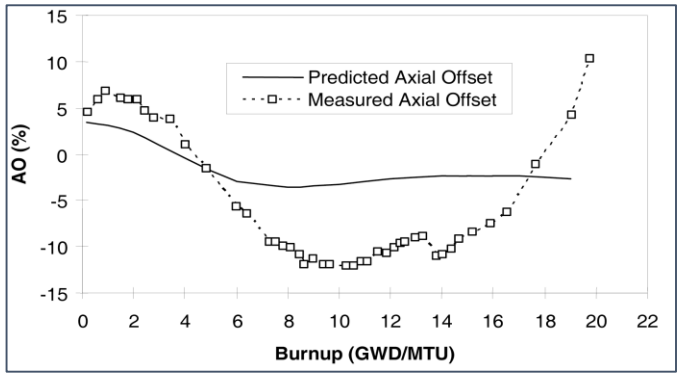

Fig CRUD induced power shift (CIPS) – Westinghouse

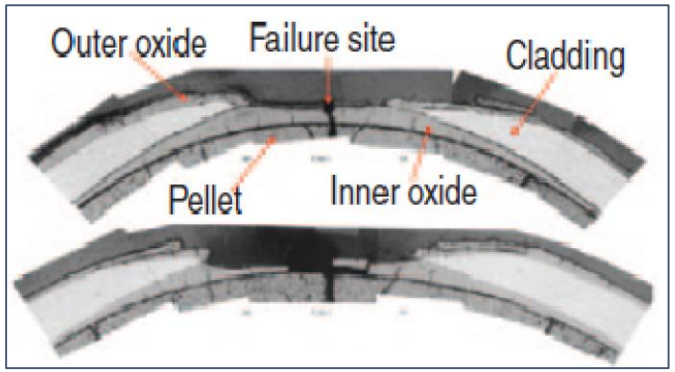

Fig CRUD induced localized corrosion (CILC)

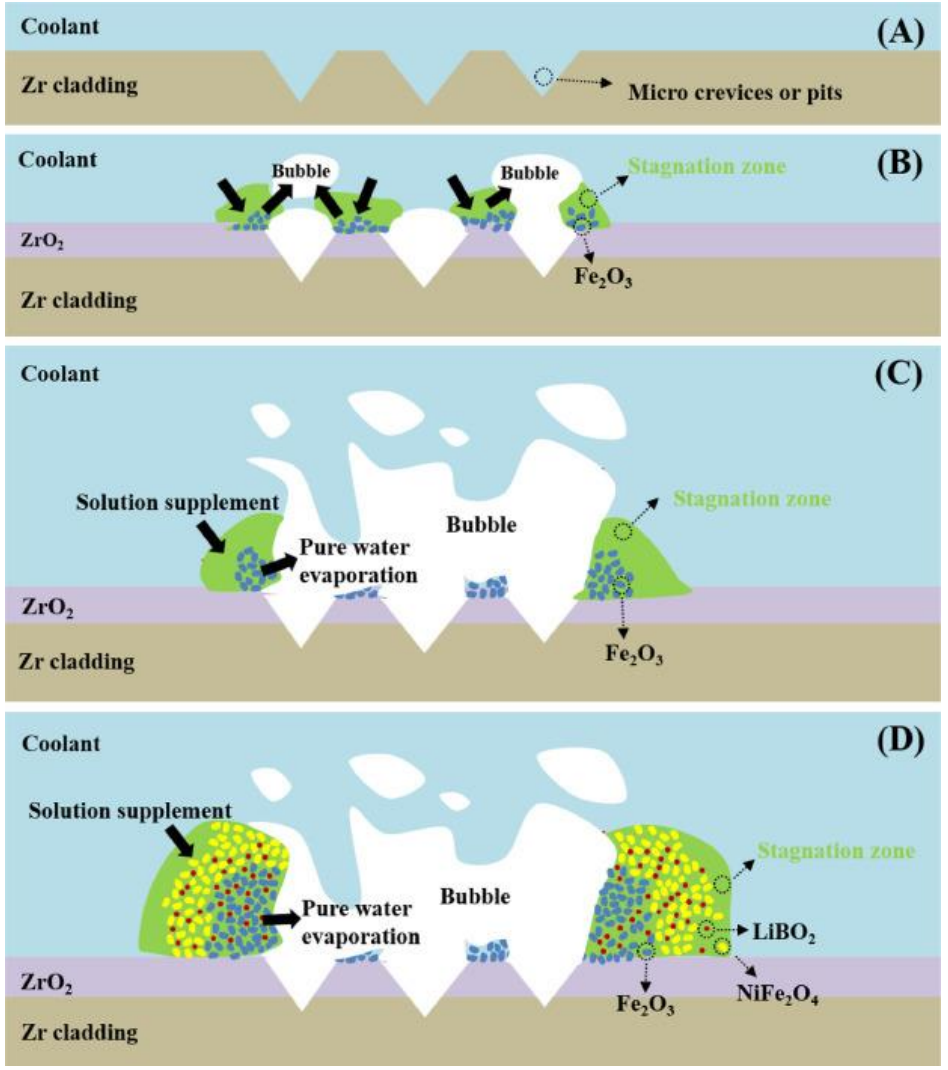

Fig Schematic diagrams of crud deposition and B enrichment mechanisms[6]

Necessity of a CRUD Source-Term model

- **Goal: ensure core stability and operational reliability under high power, long cycle operation**
  - CRUD lowers core safety and operational reliability — CIPS, CILC, and higher radiation dose
  - Corrosion products released from steam generators and piping in the primary circuit grow into CRUD[8]

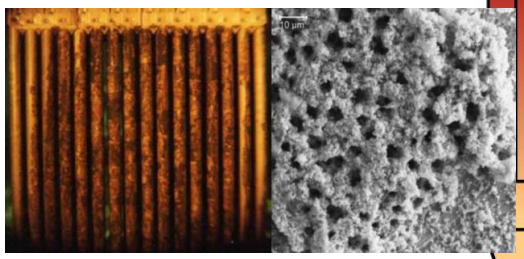

Fig Real image of CRUD deposits on the upper span of fuel[1]

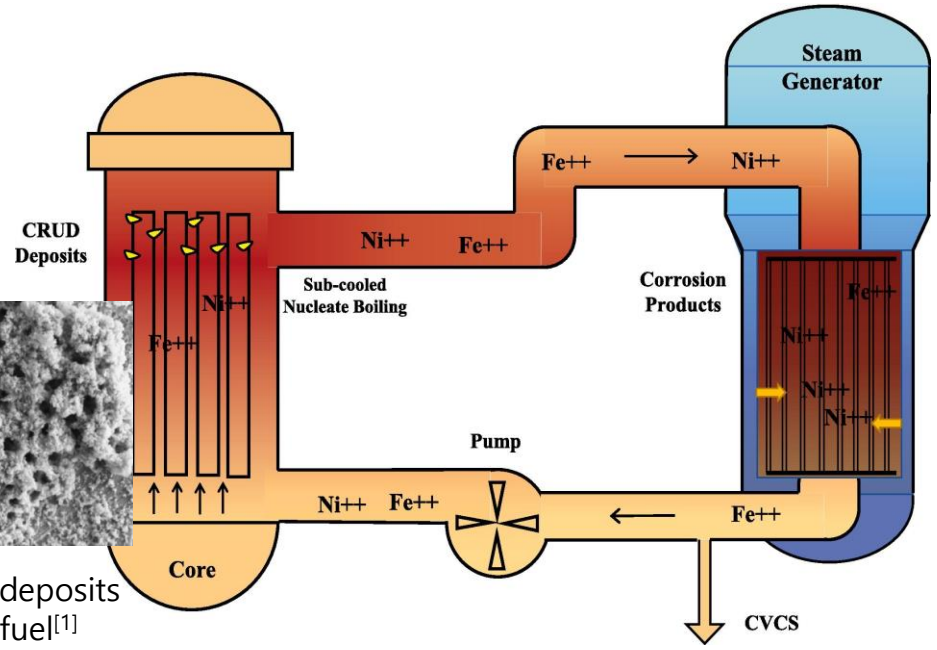

Fig Schematic of corrosion product transport and crud deposition in primary circuit of PWR[2]

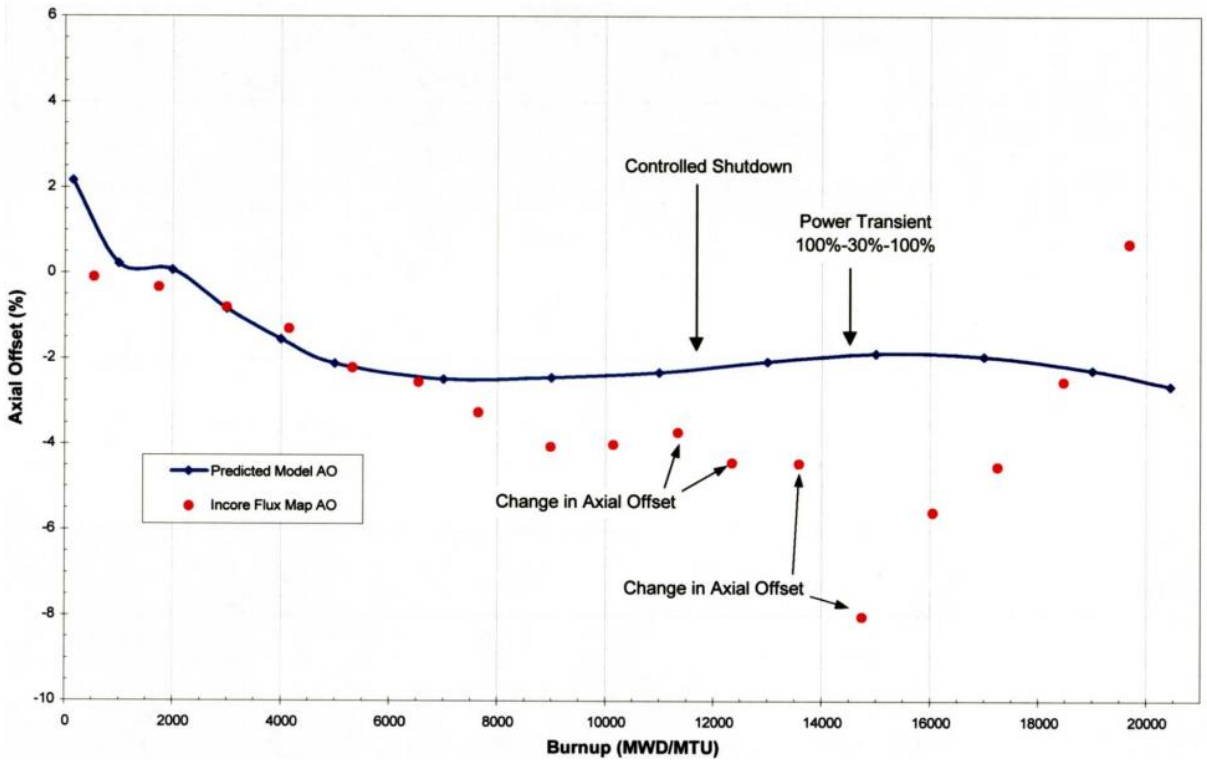

Fig Axial Offset Behavior Following Power Maneuver and Controlled Shutdown Mid-Cycle[2]

Necessity of a CRUD Source-Term model

- **Goal: ensure core stability and operational reliability under high power, long cycle operation**
  - Main source of CRUD
    - SG tubes (65–75% of RCS surface area) are the main source of corrosion products
      - Higher Cr content gives stronger corrosion resistance
  - A fraction of primary-circuit corrosion products are activated to radioactive nuclides, becoming the principal occupational radiation source

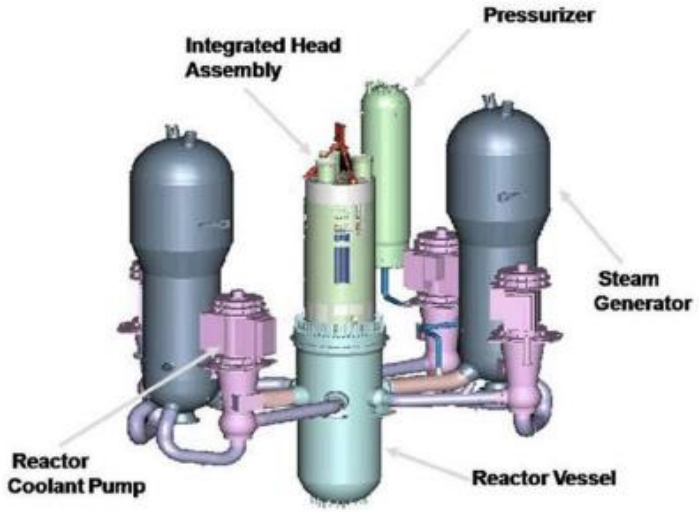

Fig Composition of Various Steam Generator Tube[9]

	Alloy 600	Alloy 690	Alloy 800
Ni, %	**72.0** (min)	**58.0** (min)	**32.0 ~ 35.0**
Fe, %	6.0 ~ 10.0	7 ~ 11	38 ~46
Cr, %	**14.0 ~17.0**	**27 ~ 31**	**19.0 ~ 23.0**

Corrosion rate: Alloy 600 > Alloy 690 ≥ Alloy 800

Fig Composition of Various Steam Generator Tube *Materials*[1]

What Is the CRUD Source Term?

What Is the CRUD Source Term?

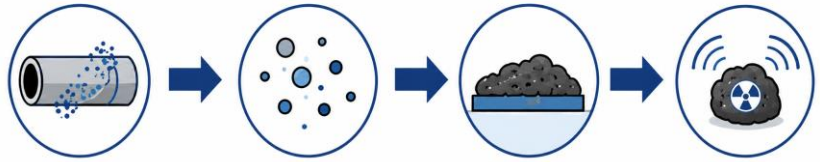

Primary-side corrosion → Metal ions / particles → CRUD formation → Radiation source

- Metal ions and particles released from primary-circuit corrosion (Fe, Ni, etc.)
- Dissolved/particulate partition is governed by equilibrium solubility
- It varies with time and operating conditions
- It is the feedstock for CRUD formation and a source of radiation/worker dose.

What a source-term model enables

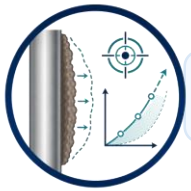

Accurate CRUD-growth prediction

Mechanism-wise quantitative analysis

Reproduction of transient spikes

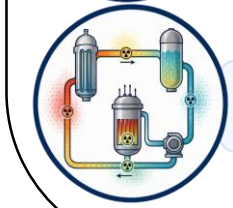

Spatial Co-58/60 distribution prediction

A CRUD source-term model is the key basis for accurate CRUD-growth prediction, activation management, and transient-operation analysis

Research Objectives

1

Objective 1

CRUD source-term model development

Develop a physics-based model to predict corrosion-product generation, transport, and source terms in the PWR primary circuit

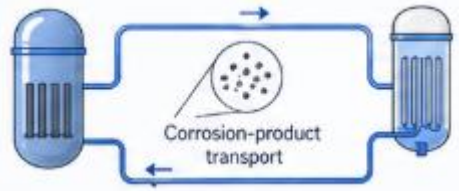

- Physics-based equations
- PWR primary system
- Corrosion-product prediction

2

Objective 2

Thermodynamic solubility surrogate model

A literature consistent thermodynamic dataset for PWR primary water + a 5-D surrogate

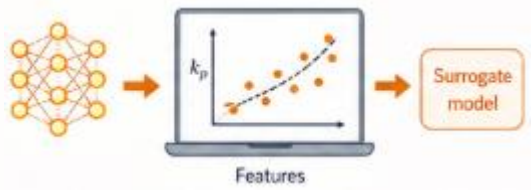

- Consistent solubility input to source term analysis
- UQ, sensitivity, and operating condition exploration

3

Objective 3

Multiphysics CRUD analysis model (future work)

Integrate thermal-hydraulics, neutronics, and CRUD chemistry into an unified Multiphysics simulation framework

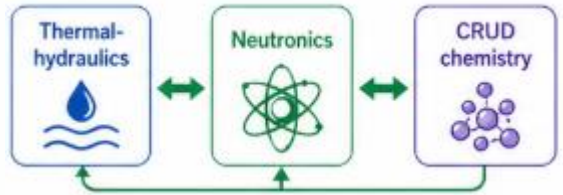

- Thermal-hydraulics coupling
- Neutronics coupling
- CRUD chemistry

Integrated outcome

A predictive coupled framework for CRUD generation, transport, deposition, boron hideout, and source-term assessment

Research Framework for CRUD-source term Model

- Four step approach

1. Feature importance and sensitivity study of CRUD growth and boron hideout

2. CRUD source term code development

3. CRUD source term code verification and validation

4. Results and discussion

Feature importance & sensitivity study of CRUD growth

- **Feature importance analysis and sensitivity study**
  - The dominant factor for CRUD thickness is the particulate concentration of corrosion products
    - Particulate source term: near-linear effect, sharp above a threshold
    - Shutdown removal: shifts the overall distribution.
    - Initial porosity: thickness increases with porosity
    - Chimney density: smallest relative effect

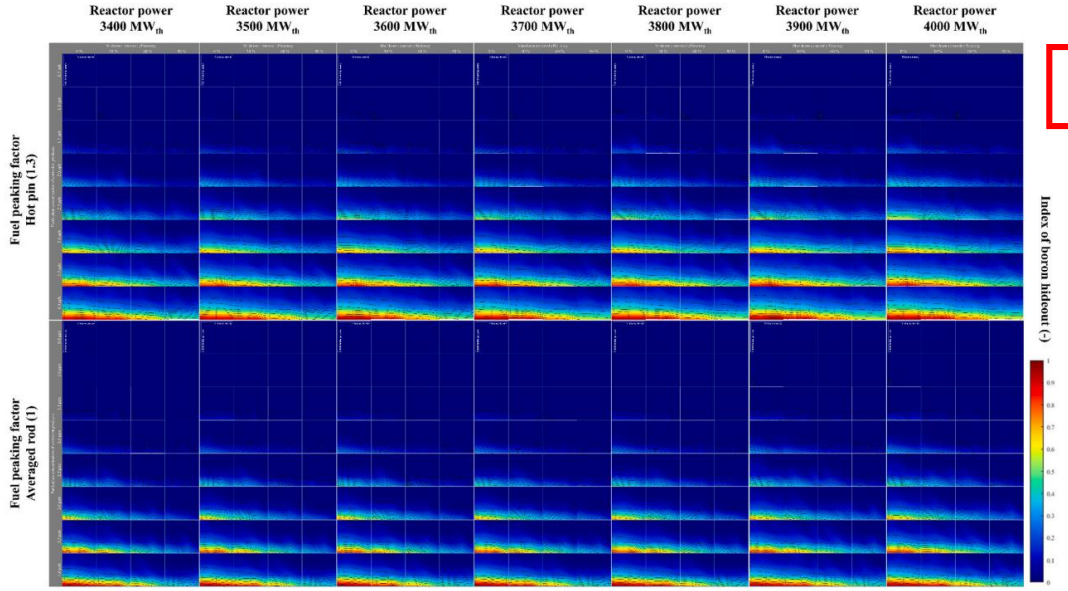

Fig Index of boron hideout evaluated for various chimney density (inner x-axis CRUD initial porosity (inner y-axis), shutdown removal efficiency (middle xaxis), particulate concentration of corrosion products (middle y-axis), reactor power level (outer x-axis) and fuel power peaking factor (both averaged rod (factor 1.0) and hot pin (factor 1.3), outer y-axis[8]

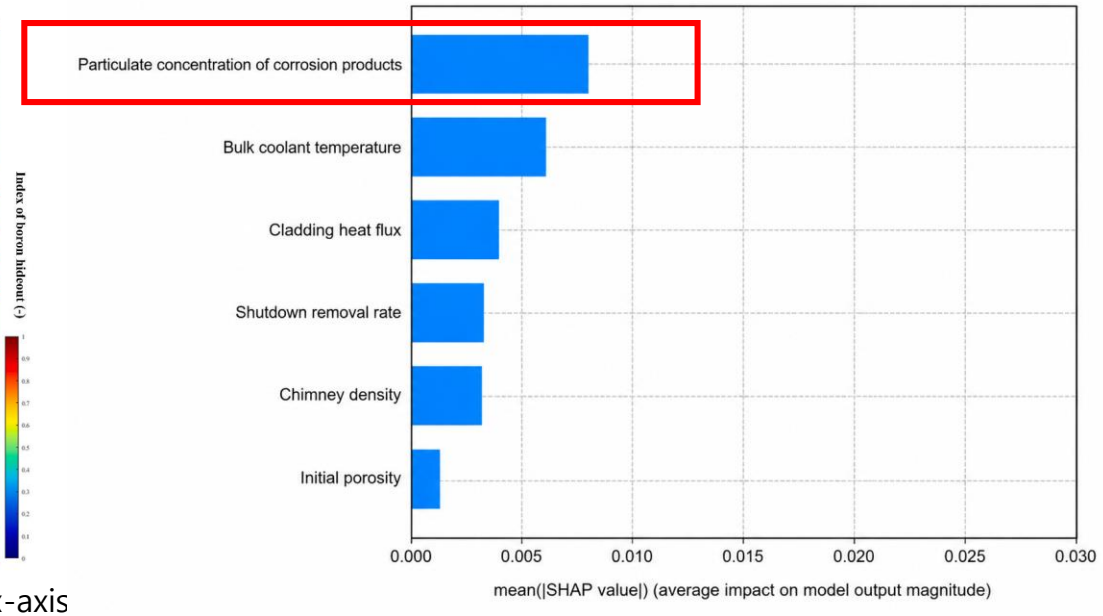

Fig Feature Importance for CRUD thickness

CRUD source term code development

▪ Research strategy and scope

1 Purpose

- Predict corrosion-product behavior in the PWR primary circuit
- Fe/Ni from structural materials are transported by coolant and deposit on fuel as CRUD

2 Target system

- Korean APR1400 / OPR1000 primary circuit
- Pressure: 15.5MPa
- RCS inlet 295℃, outlet 330℃
- Primary-circuit volume : 334.9 m^3
- SG surface area: 9,522.6 m^2

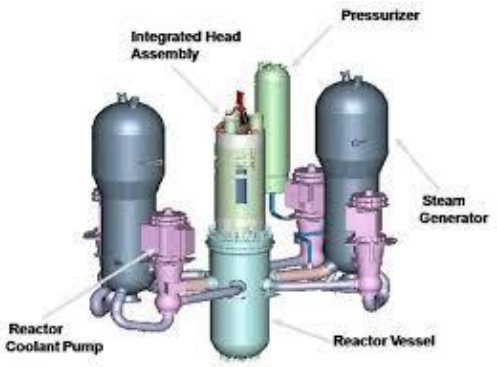

3 Key concepts

Transport of dissolved species and colloid/flake particles by coolant

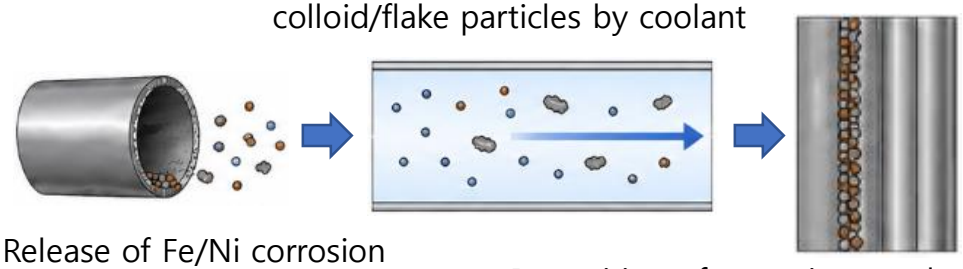

Release of Fe/Ni corrosion products from materials

Deposition of corrosion products as CRUD on fuel surface

Model assumptions

1. Each control volume is well-mixed (Re > 10^4)
2. Particulates split into colloids (< 0.45 μm) and flake(> 0.45 μm)
3. Reducing environment (radiolysis species not considered)
4. Ni/NiO is reduced (no independent NiO precipitation)

CRUD source term code development

- **Source term code architecture**
  - PWR primary circuit simplified into 16 nodes
    - Each node: volume, surface area, material, temperature, hydraulic diameter
  - Lumped model — tracks loop-average behavior, not CFD
  - 16 nodes × 25 variables = 400 ODEs
    - Tracks dissolved Fe/Ni, particulate Fe/Ni, related species, water chemistry, and T
  - Operator-splitting integration implemented with solubility surrogate model
  - Computation using Python (NumPy/SciPy)

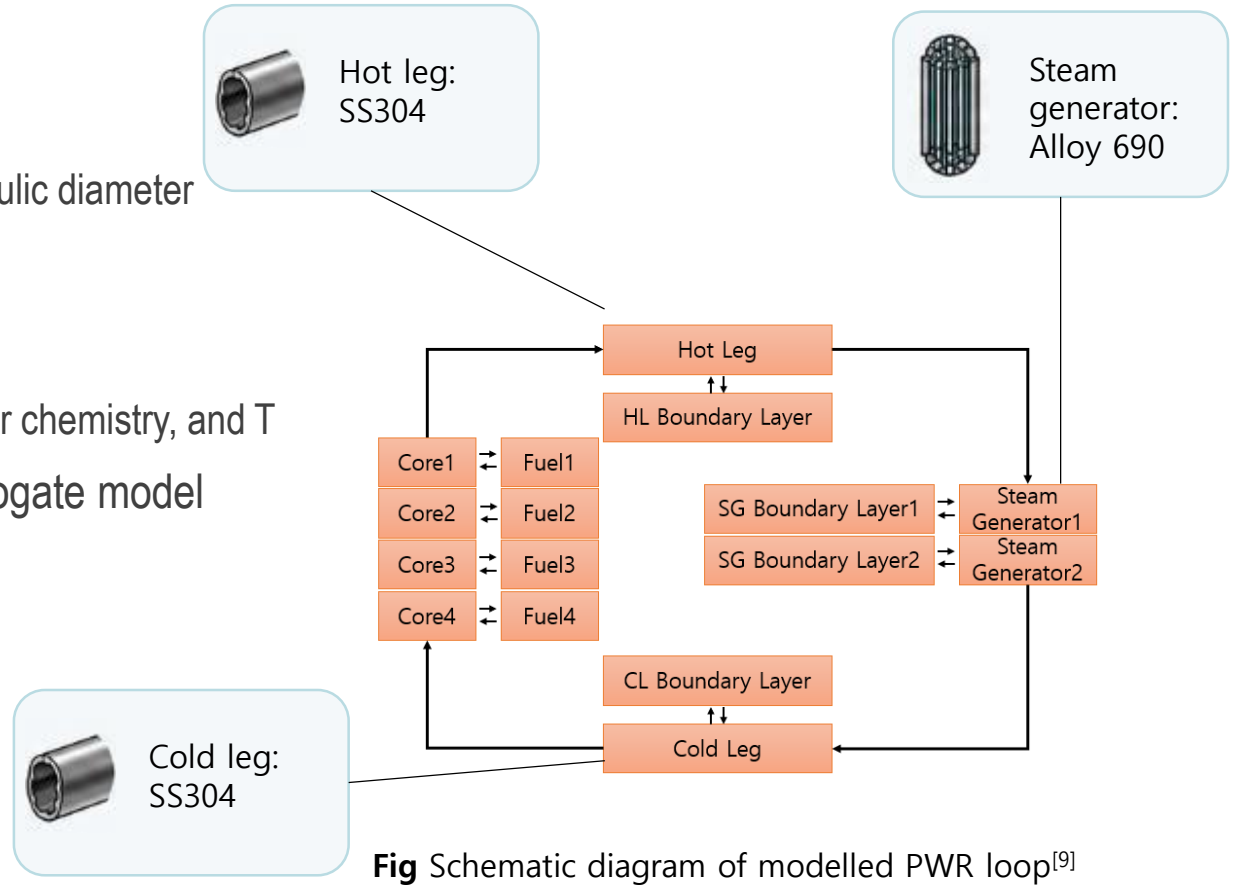

Fig Schematic diagram of modelled PWR loop[9]

CRUD source term code development

- **Source term code architecture**
  - Node-wise modeling of thermal-hydraulics, oxide growth, corrosion release, solubility, particle nucleation/erosion/deposition and CVCS purification(operator splitting)
  - Dissolved-species mass balance: corrosion release + dissolution + transport − precipitation − purification

$$V_j \frac{dC_{i,j}}{dt} = J_{rel,i}A_j + \dot{Q}\left(C_{i,in} - C_{i,j}\right) - R_{prec,i}A_j - \dot{Q}_{pur}\beta_i C_{i,j} + J_{diss,i}A_j$$

  - Inner-oxide inventory

$$\frac{dm_{in,i,j}}{dt} = J_{growth,i,j} - J_{rel,i,j}$$

  - Outer-oxide inventory

$$\frac{dm_{out,\phi,j}}{dt} = R_{prec,\phi} + R_{dep,\phi} - R_{eros,\phi} - R_{diss,\phi} - R_{comp,\phi}$$

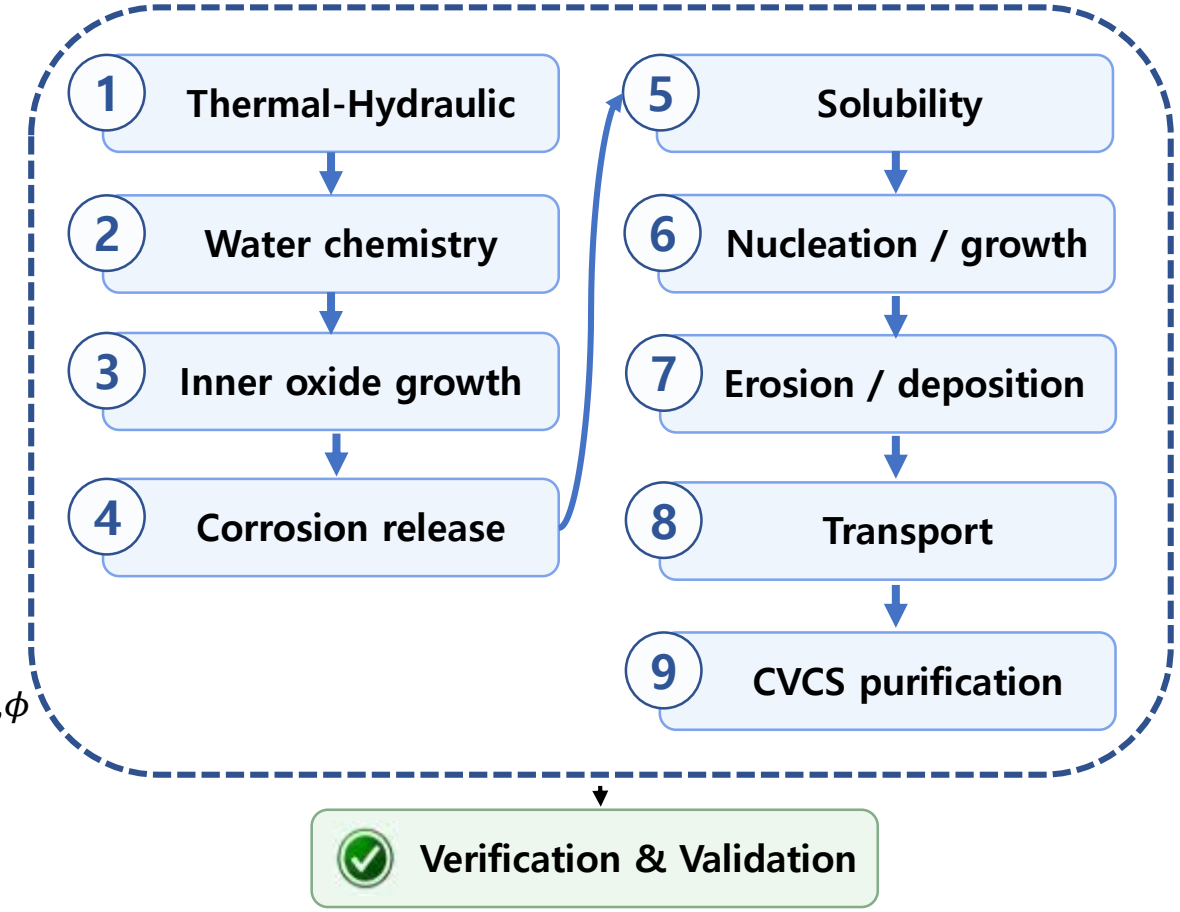

CRUD source term code development

▪ Thermal-hydraulic and pH model

0 Role

- T and pH are inputs to corrosion, precipitation, and transport modules

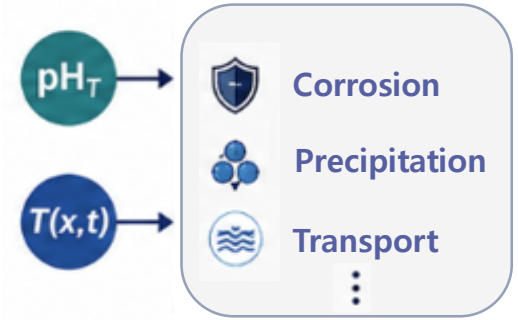

2 Water chemistry / pH

$$\log K_\omega = A + \frac{B}{T} + \frac{C}{T^2} + \frac{D}{T^5} + \left(E + \frac{F}{T} + \frac{G}{T^2}\right) log\rho_\omega$$

Marshall-Frank

$$\mathrm{p}K_a(T) = \frac{2948}{T} - 13.249 + 0.04196T$$

Mesmer et al.

$$\log\gamma_i = -A_{DH} z_i^2 \frac{\sqrt{I}}{1 + B_{DH} \mathring{a}_i \sqrt{I}} + \dot{B} I$$

Debye-Hyckel Theory

1 Thermal-Hydraulic

$$(\rho V C_p)_j \frac{dT_j}{dt} = \dot{m} C_p (T_{in,j} - T_j) + Q_{gen,j} - Q_{loss,j}$$

$$\frac{1}{h_{eff}} = \frac{1}{h_{conv}} + \frac{\delta_{dep}}{k_{eff}}$$

Effective heat-transfer coefficient

$$Nu = 0.023 Re^{0.8} Pr^{0.4}$$

Dittus-Boelter

$$k_{eff} = k_f [2k_f + k_s - 2\varphi(k_f - k_s)] / [2k_f + k_s + \varphi(k_f - k_s)]$$

Maxwell-Eucken model

CRUD source term code development

- **Inner oxide growth and corrosion release**

3 Wagner oxide growth

$$\frac{dx}{dt} = \frac{k_p(T)}{2x}$$

$$k_p(T) = Aexp(-Q/R\,T)$$

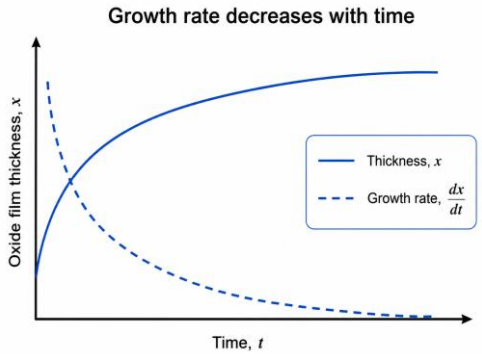

- Wagner's law: thickness $x \propto \sqrt{t}$
- As thickness grows δ_{eff} increases $J_M \propto \frac{1}{\delta_{eff}}$ decreases
- Fe and Ni release decrease with time

4 Fickian corrosion release

$$J_M = \frac{D_{eff}(T)}{\delta_{eff}}(C_{interface} - C_{bulk})$$

$$D_{eff}(T) = D_0 r_{eff}(\varphi_{lab}, \varphi_{FeCr}, \varphi_{Cr})\exp(-Q_D/\mathrm{R\,T})$$

$$C_{interface} = w_{M,alloy} C_{M,ref}$$

- As the Cr-protective fraction grows, r_{eff} decreases
- Lower D_{eff} and higher protectiveness make diffusion harder
- As a result, Fe and Ni release decrease in a self-limiting way

CRUD source term code development

- **Solubility, nucleation, and crystal growth**

5 Solubility & supersaturation

$$\Delta G^{\circ}_{rxn} = -RTlnK$$

$$logK_{sp} = -\frac{\triangle G^{\circ}_{rxn}}{2.303RT}$$

$$Fe_3O_4(s) + 6H^+(aq) + H_2(g) \rightleftharpoons 3Fe^{2+}(\mathrm{aq}) + 4H_2O(l)$$

$$\mathrm{Ni}Fe_2O_4(s) + 6H^+(aq) + H_2(g) \rightleftharpoons Ni^{2+}(\mathrm{aq}) + 2Fe^{2+}(\mathrm{aq}) + 4H_2O(l)$$

$$C_{total} = C_{free}(1 + \beta_1[OH^-] + \beta_2[OH^-]^2)$$

6 Nucleation

$$S = \frac{C}{C_{sat}} > 1$$

$$\Delta \mathrm{G(r)} = \left(\frac{4}{3}\right)\pi r^3 \Delta G_v + 4\pi r^2 \gamma$$

$$r^* = -2\gamma / \Delta G_v$$

$$\Delta G^* = 16\pi\gamma^3 / 3\,\Delta G_V^2$$

$$J_{nuc} = J_0 \exp\left(-\frac{\Delta G^*}{k_B T}\right)$$

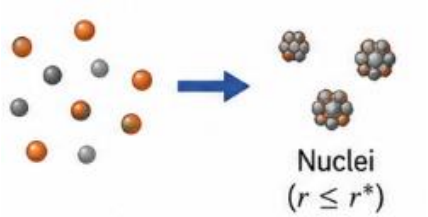

6 Crystal growth

$$\frac{dm}{dt} = k_g S_p (C - C_{sat})$$

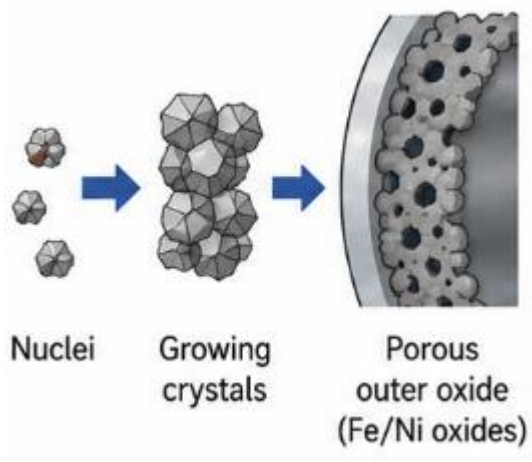

CRUD source term code development

- **Inner oxide growth and corrosion release**

7 Erosion

$$\tau_w = f\frac{1}{2}\rho v^2$$ Fanning

$$R_{eros} = k_e(\tau_w - \tau_{crit})m_{deposit} \quad (\tau_w > \tau_{crit})$$

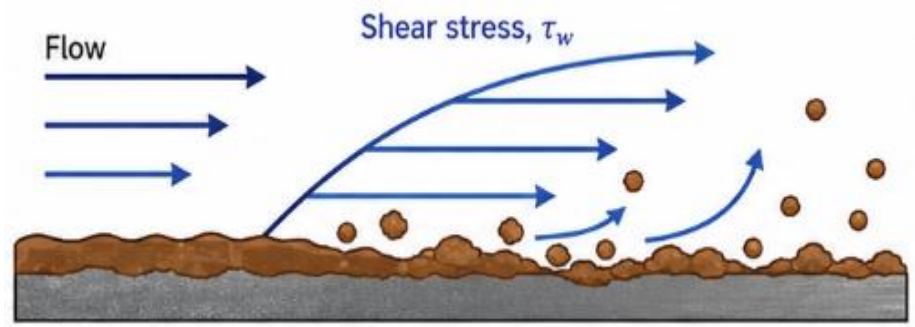

7 Particle–surface attachment

$$W_{ad} = \frac{A_H R}{12\delta_0^2}$$ DMT model

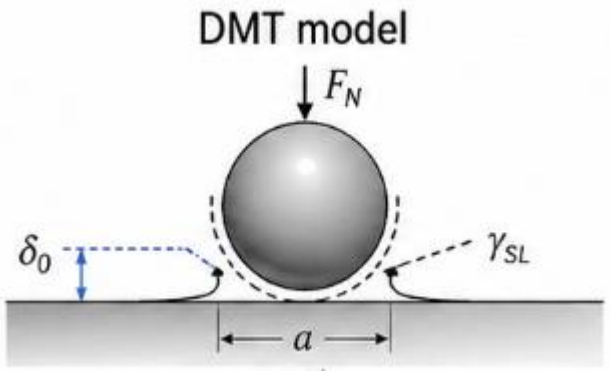

8 Transport

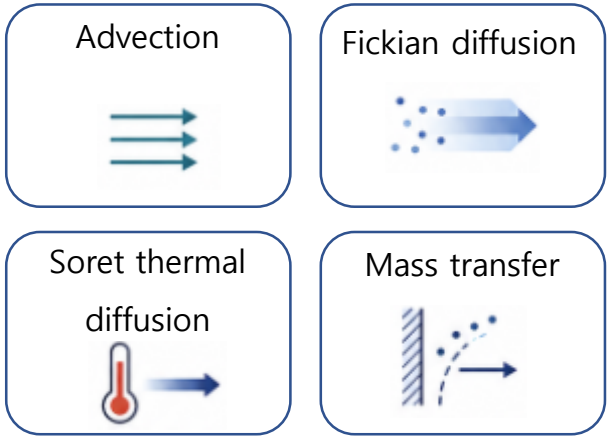

$$\frac{dC_{i,j}}{dt} = (\frac{1}{\tau_j})(C_{i,in} - C_{i,j})$$

$$-D\frac{\partial C}{\partial z} \qquad -D\frac{\partial T}{\partial z}$$

CRUD source term code development

- **CVCS purification system**

9 Purification

$$\frac{dC_i}{dt} = -(\frac{\dot{Q}_{pur}}{V})\beta_i C_i$$

$$f_{pur} = \frac{\dot{Q}_{pur}}{\dot{Q}_{loop}}$$

- CVCS reduces the corrosion-product concentration in the coolant
- A larger purification flow ($\dot{Q}_{pur}$) gives more removal
- Purification ratio(f_{pur}) sets the overall purification strength

Species type	β	Removal mechanism
Dissolved ions (Fe^{2+}, Ni^{2+}, etc.)	0.90	mixed-bed ion exchange
Colloids (< 0.45 μm)	0.40	partial filtration
Flakes (> 0.45 μm)	0.90	mechanical filtration

Fig Removal efficiency β by species type

Thermodynamic Solubility Surrogate Modeling

▪ Why PWR specific solubility data?

1 Key message

- PWR source-term depends on equilibrium solubility of Fe/Ni oxides and spinels
- Default LLNL underpredicts magnetite solubility by ~ 100~1000x
- Literature data also scatter by ~6x
- A PWR-specific thermodynamic input dataset is therefore required

2 Scope

- T: 250 ~ 330℃ (Extrapolated: 300 ~ 330 ℃)
- pH_T: 6.7 ~ 7.4
- C_{H_2}: 25 ~ 50 cc/kg
- P: 15.5 MPa

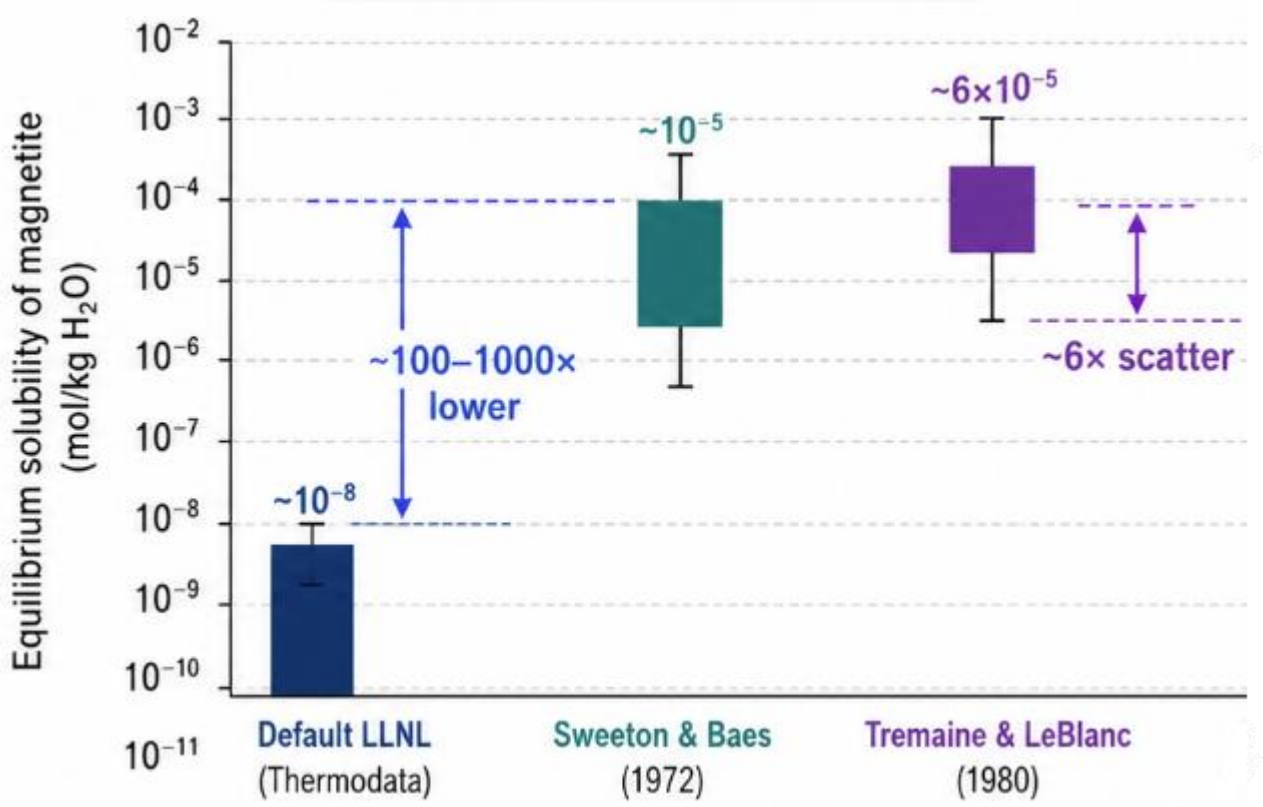

Fig Magnetite solubility comparison

Thermodynamic Solubility Surrogate Modeling

- **Coupling the surrogate with the source-term model**

1 Key message

Thermodynamic dataset for PWR primary water + a 5-D surrogate, coupled to the source-term code, deliver a consistent solubility input

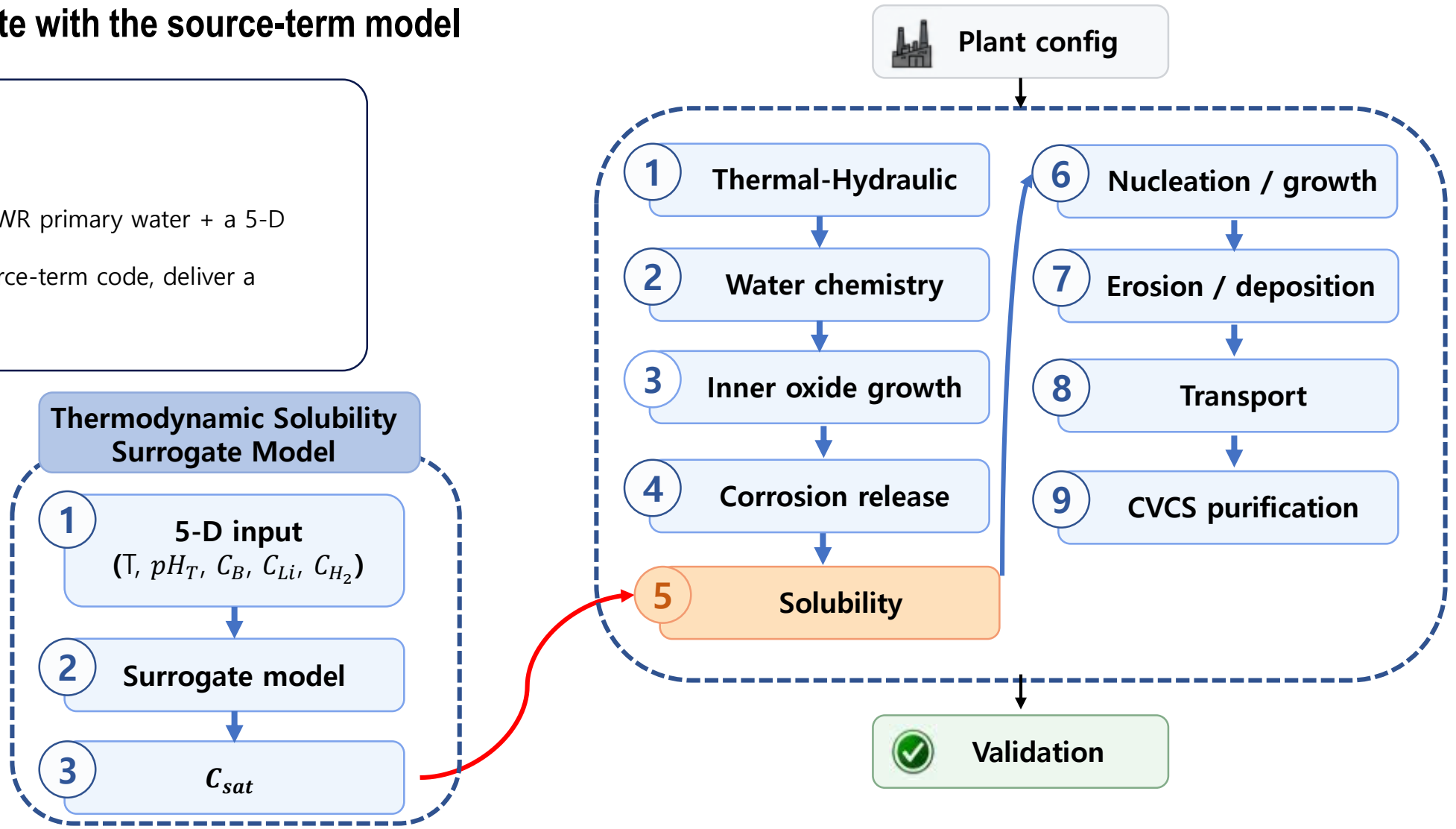

SNUCRUST: Results

- **Evaluation items**
  - Inner-oxide growth, Fe/Ni corrosion release, outer-oxide growth and composition, dissolution–precipitation balance, particulate corrosion-product behavior, comparison with measured plant concentrations

SNUCRUST: Results

- **[Corrosion growth stage] SS304 inner oxide(cold leg, hot leg)**
  - (Literature) $FeCr_2O_4$ chromite spinel is dominant (TEM/STEM results)[10]
  - (Literature) Composition: Fe-Cr spinel (60-80%), thin Cr-rich layer[11]
    - (SNUCRUST) In the cold leg, $FeCr_2O_4$ accounts for ~80%, $FeCr_2O_4$ ~ 19%, Cr_2O_3 ~2% (at 500 days)

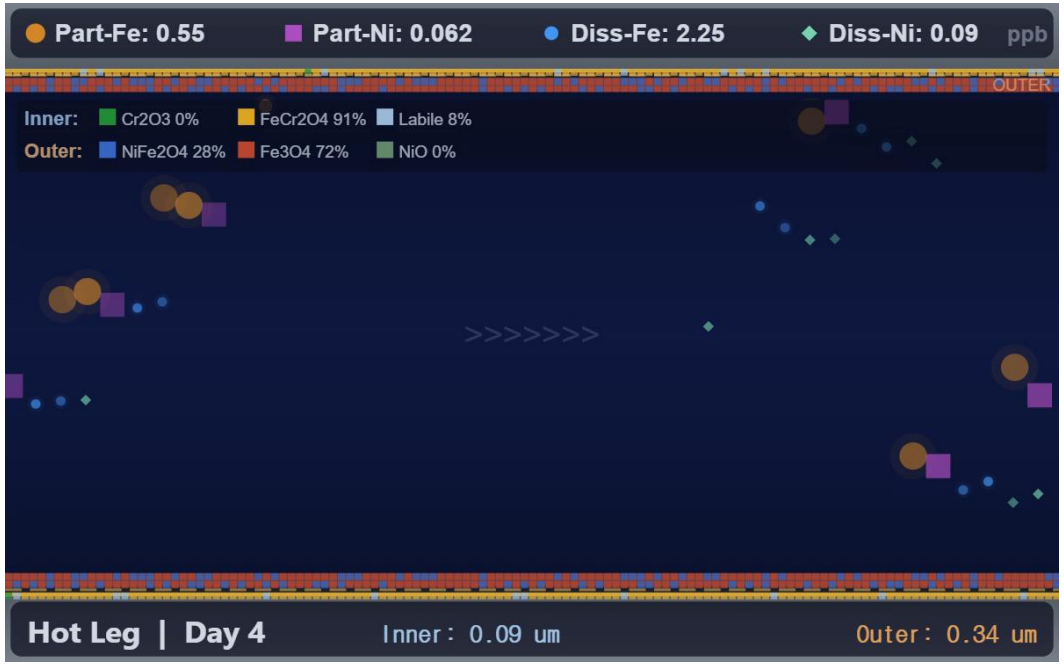

SNUCRUST: Results

- **[Corrosion growth stage] Alloy 690 inner oxide (steam generator)**
  - (Literature) $(Ni, Fe)Cr_2O_4$ chromite spinel is the main phase, with discontinuous ~5 nm Cr_2O_3 at grain interfaces
  - (Literature) The 30% Cr increases the thermodynamic stability of Cr_2O_3, but under PWR conditions the chromite spinel is dominant and Cr_2O_3 exists only as discontinuous ~5 nm grains at grain interfaces
    - (SNUCRUST) In SG inlet, Cr_2O_3 accounts for 95~97%($FeCr_2O_4$ ~ 40%, $FeCr_2O_4$~ 56%), Cr_2O_3 3~5% (at 500 days)

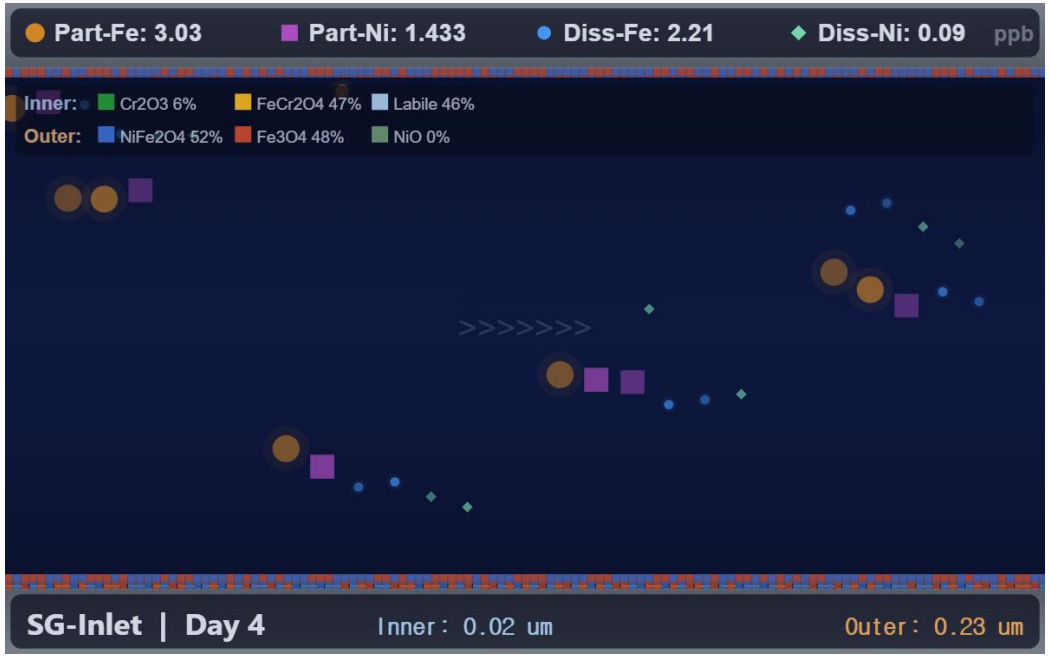

SNUCRUST: Results

- **[Corrosion growth stage]**
  - Inner-oxide thickness grows monotonically at all nodes

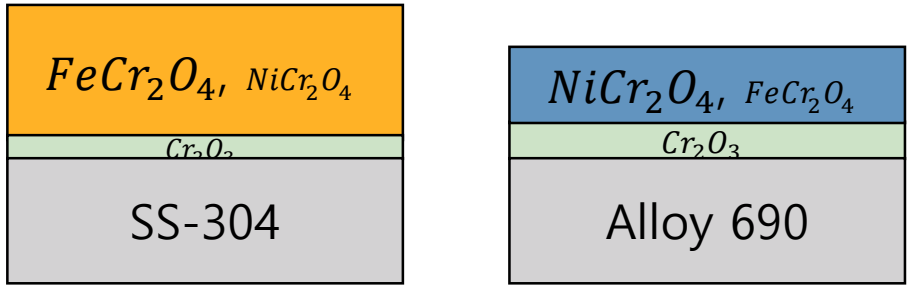

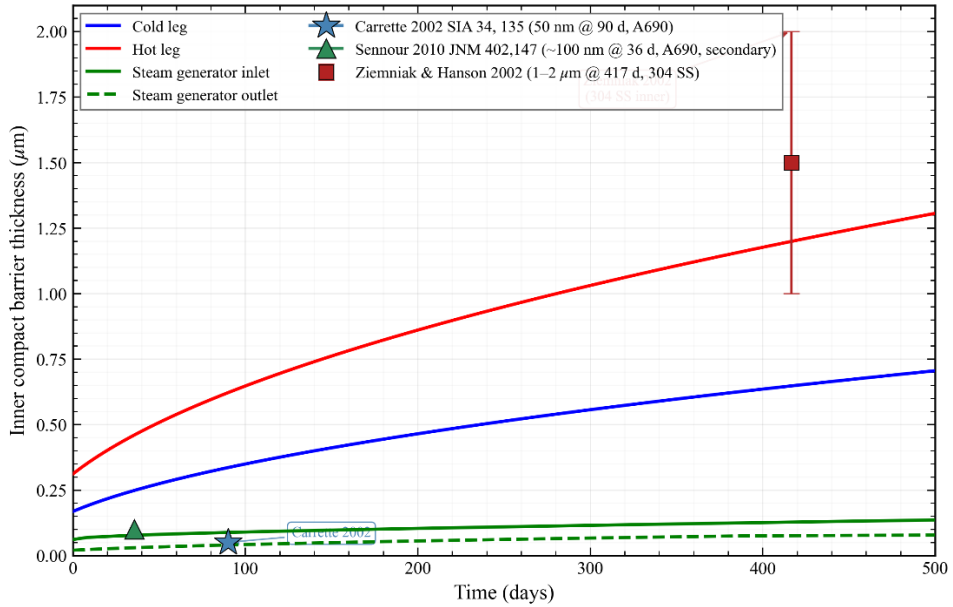

    - SS-304 develops a thicker inner oxide layer than Alloy 690.
    - SS-304 forms a $FeCr_2O_4$ -dominant inner layer.
    - Alloy 690 forms a $NiCr_2O_4$ $-dominant$ inner layer.
    - Alloy 690 forms a Cr_2O_3 $-$ rich protective layer.
  - The oxide film thickness is in the experimental ranges reported by Sennour, Carrette, and Ziemniak

Interpretation

Lower Cr
Higher Fe
(SS-304)

→ faster growth ↑

lower protective barrier effect
$FeCr_2O_4 - dominant\ inner\ layer$

Higher Cr
Higher Ni
(Alloy 690)

→ ↓ Slower growth

higher protective barrier effect
$NiCr_2O_4$ –dominant inner layer

SNUCRUST: Results

- **[Corrosion growth stage]**

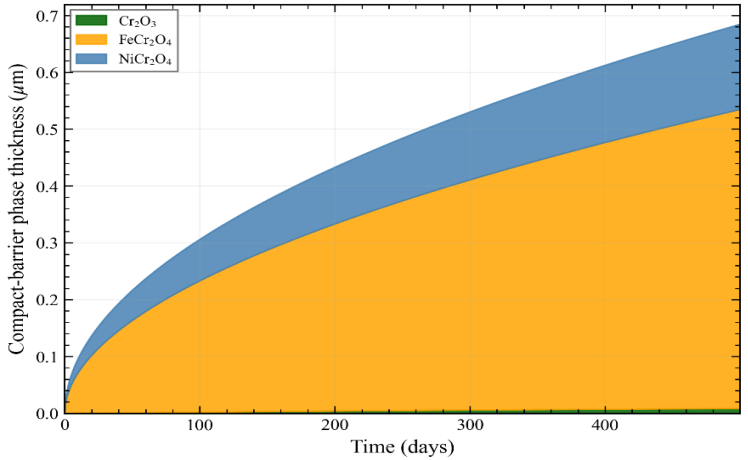

Fig Time Evolution of Inner-Layer Oxide Phase Fractions under Cold-Leg Conditions

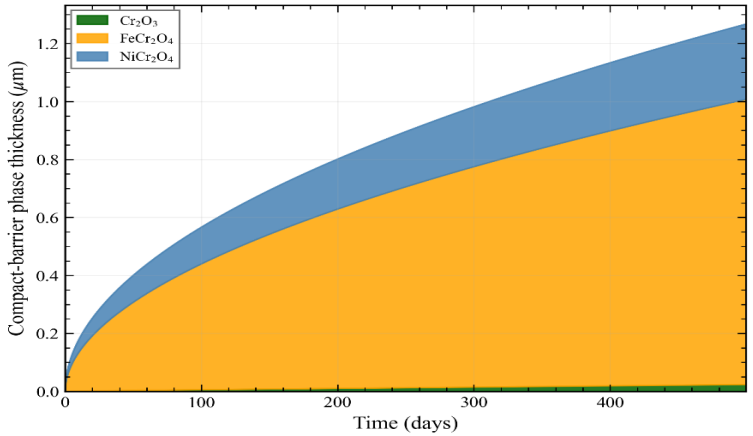

Fig Time Evolution of Inner-Layer Oxide Phase Fractions under Hot-Leg Conditions

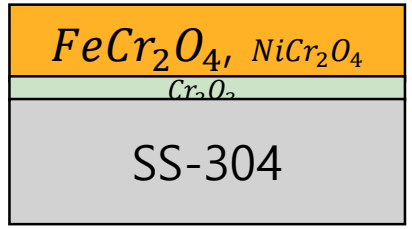

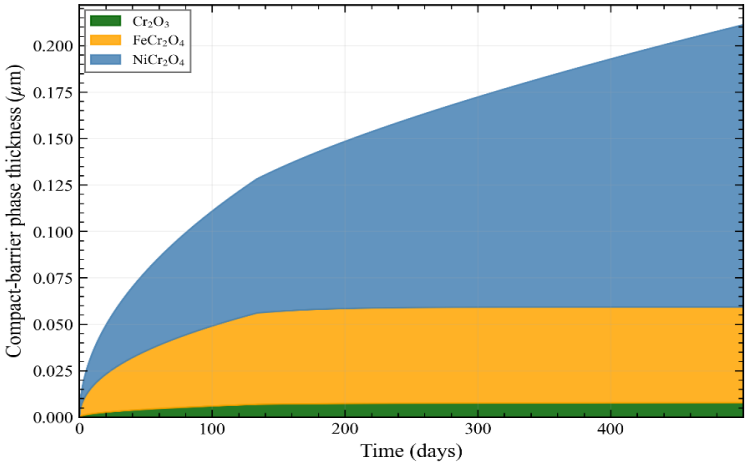

Fig Time Evolution of Inner-Layer Oxide Phase Fractions at the Steam-Generator Inlet

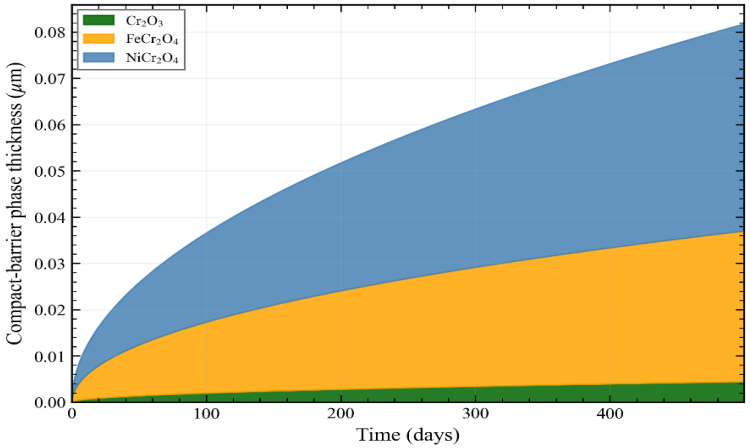

Fig Time Evolution of Inner-Layer Oxide Phase Fractions at the Steam-Generator Outlet

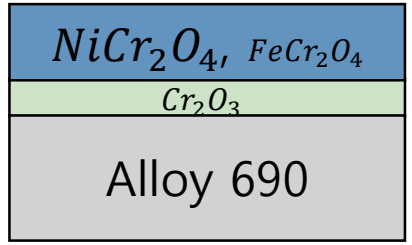

SNUCRUST: Results

- **[Corrosion release stage]**
  - Inner oxide thickness follows $\delta(t) \propto \sqrt{t}$, leading to flux behavior $J \propto 1/\sqrt{t}$ [12, 14]
  - Fe release per unit area
    - SS-304: $J_{Fe} \approx 1.4 \sim 2.6 \times 10^{-12}\ mol/m^2/s$
    - Alloy-690: $J_{Fe} \approx 3.4 \sim 4.2 \times 10^{-13}\ mol/m^2/s$
  - Alloy 690 lower Fe release due to its Cr-rich protective layer
  - But the SG has a very large surface area, so the absolute release is still large

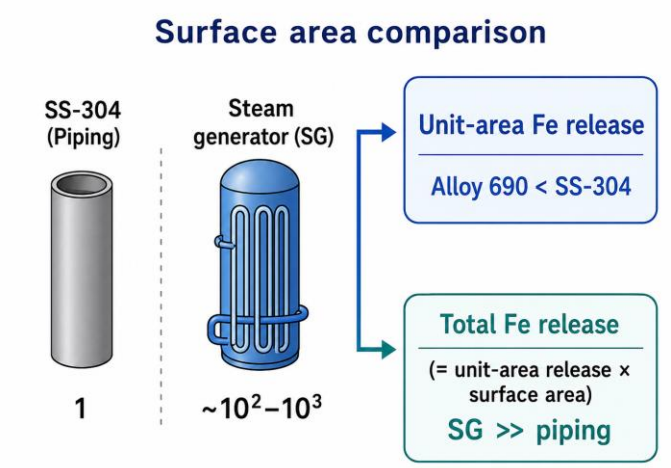

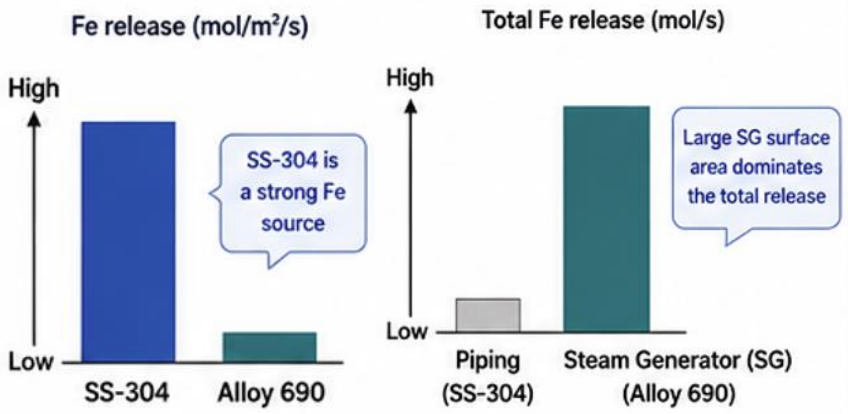

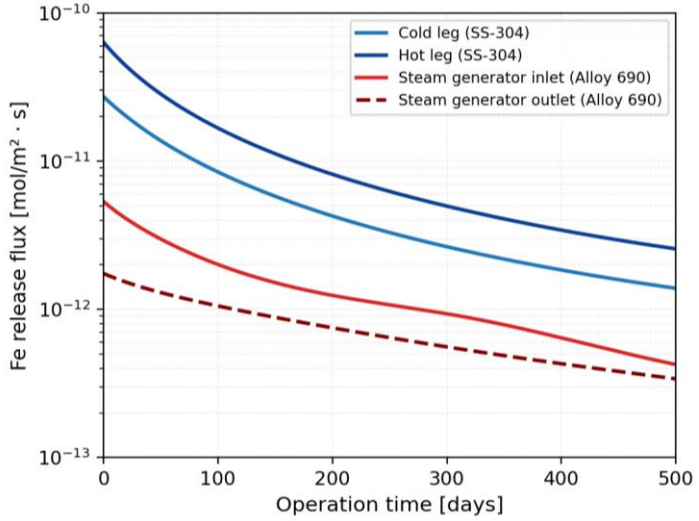

Fig Time Evolution of Per-Unit-Area Fe Release Flux by Location

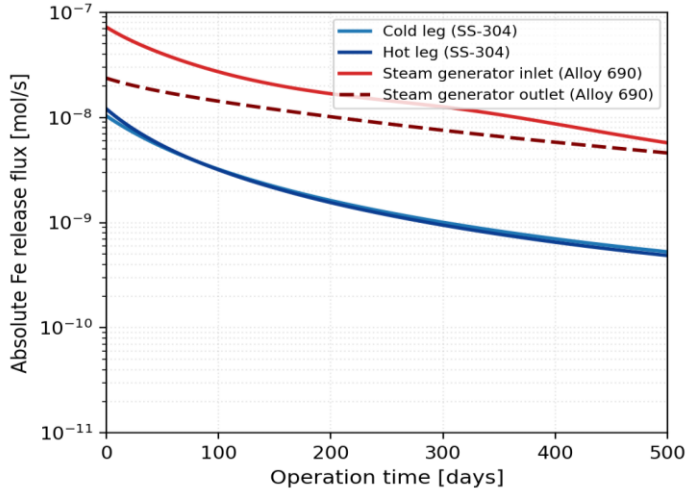

Fig Time Evolution of Total Fe Release Flux by Location in the PWR Primary Coolant System

SNUCRUST: Results

- **[Corrosion release stage]**
  - Ni release per unit area
    - SS-304: $J_{Ni} \approx 2.1 \sim 4.2 \times 10^{-14}\ mol/m^2/s$
    - Alloy-690: $J_{Ni} \approx 4.4 \sim 6.2 \times 10^{-13}\ mol/m^2/s$
  - Ni release is higher for Alloy 690 because of its higher Ni content

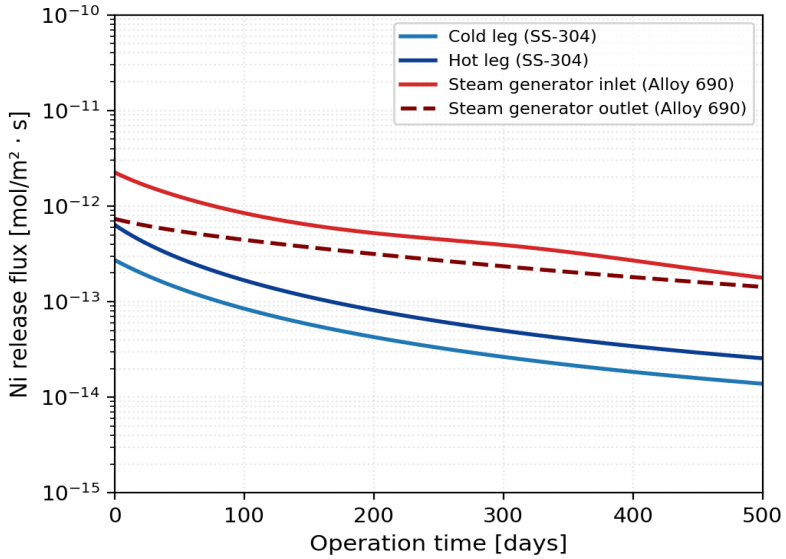

Fig Time Evolution of Per-Unit-Area Ni Release Flux by Location

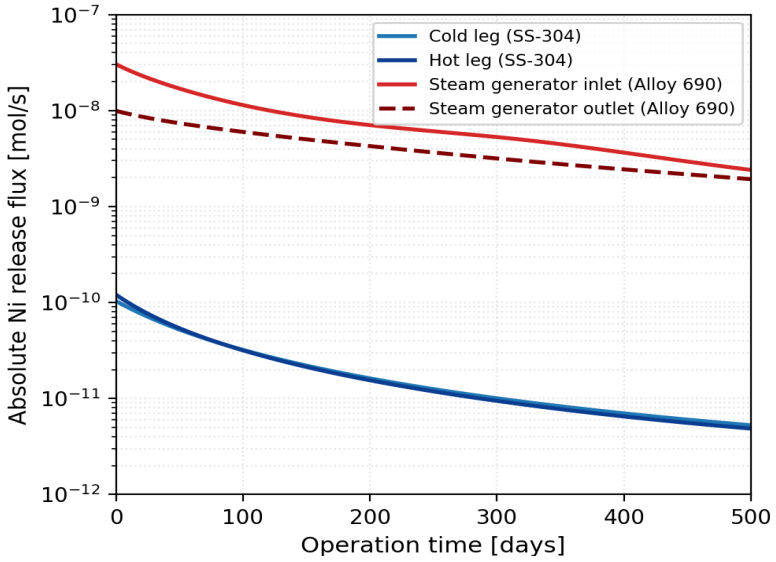

Fig Time Evolution of Total Ni Release Flux by Location in the PWR Primary Coolant System

SNUCRUST: Results

- **[Particulate formation & outer oxide layer growth stage]**
  - $\delta_{HL} \approx 0.943\ \mu m > \delta_{HL} \approx 0.588\ \mu m > \delta_{HL} \approx 0.579\ \mu m\ > \delta_{HL} \approx 0.321\ \mu m$
    - HL is thickest: lower magnetite solubility at higher T → more supersaturation
    - SG outlet is thinnest: Alloy 690 Fe release per area is ~1/6 of SS-304 → Fe-supply limited

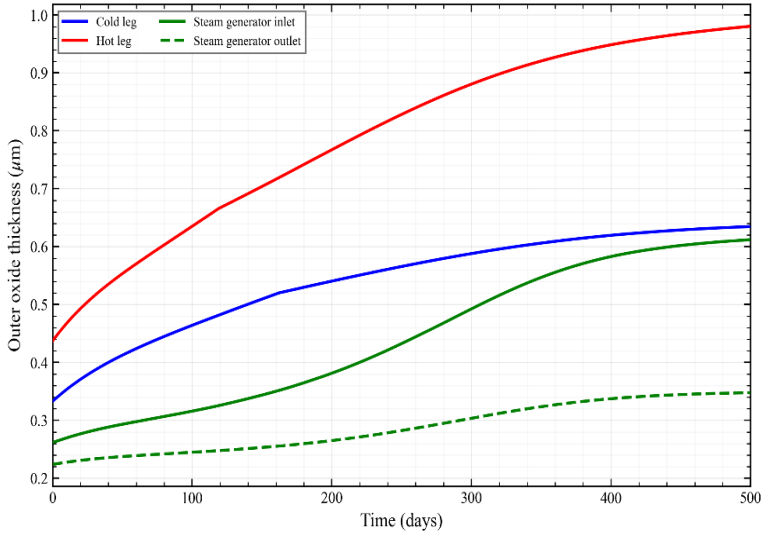

Fig Outer-Layer Oxide Growth Behavior on Structural Materials by Location in the PWR Primary Coolant System

SNUCRUST: Results

- **[Particulate formation & outer oxide layer growth stage]**
  - Outer oxide forms as a $NiFe_2O_4 - Fe_3O_4$ spinel
  - Predicted Ni : Fe atomic ratio = 0.29–0.38.
    - Consistent with XRD/EDS reports (0.20–0.50)
  - NiO is not formed under reducing PWR conditions
  - $NiFe_2O_4\ fraction: sg\ inlet > hot\ leg > cold\ leg > sg\ outlet$
    - Inverse solubility: lower T → higher Fe_3O_4 fraction

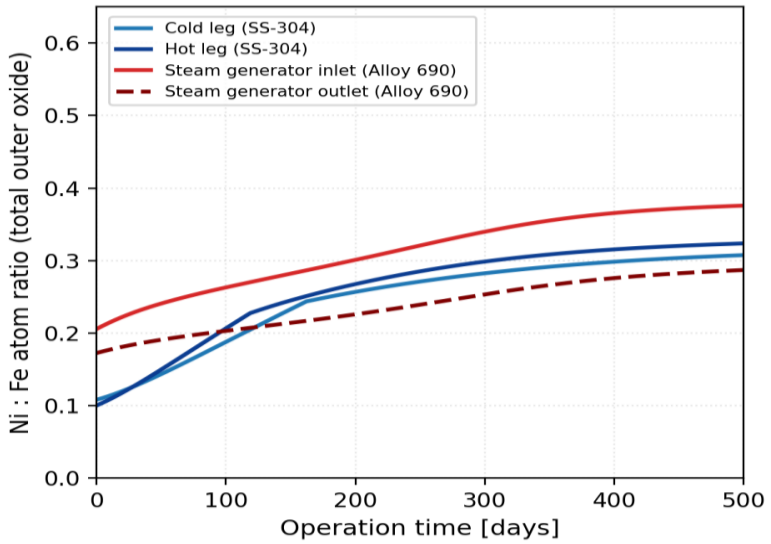

Fig Variation of the Ni:Fe Atomic Ratio in the Outer-Layer Oxide by Location

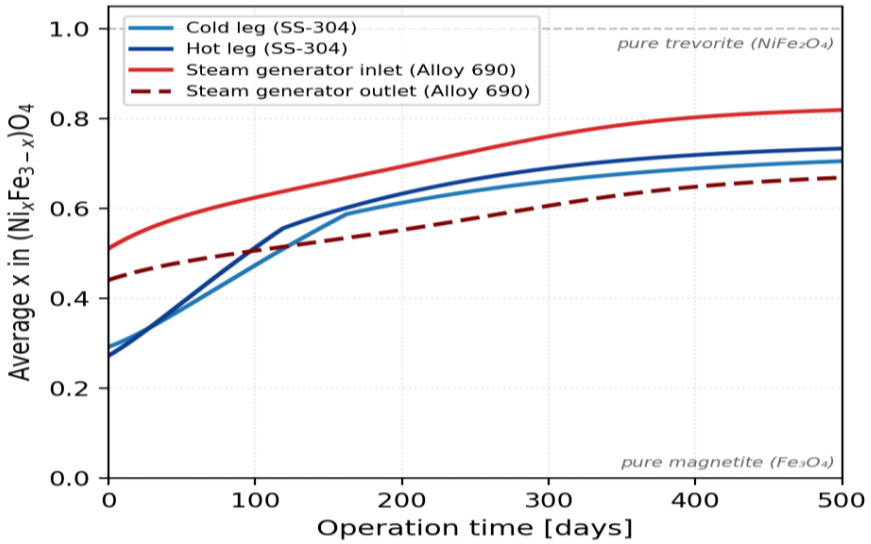

Fig Variation of the Ni Substitution Fraction (x) in the Outer-Layer Spinel Oxide by Location

SNUCRUST: Results

- **[Particulate formation & outer oxide layer growth stage]**

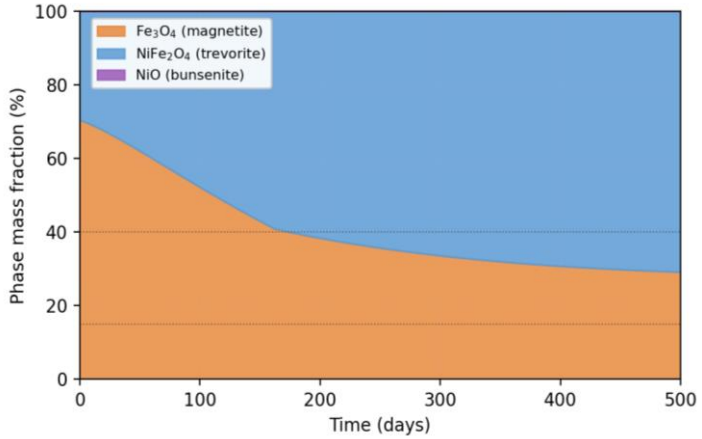

Fig Time Evolution of Outer-Layer Oxide Phase Fractions on SS-304 under Cold-Leg Conditions

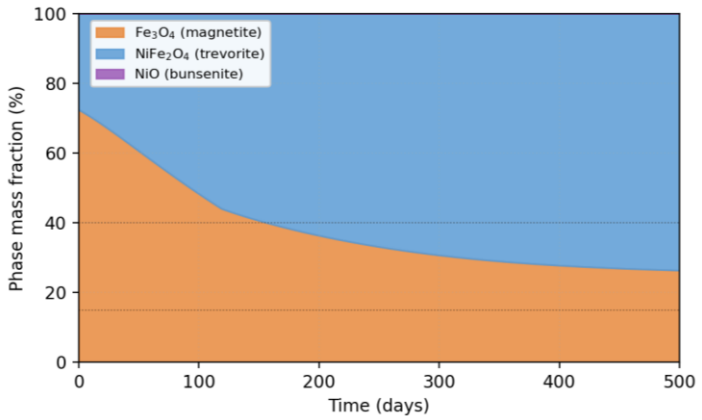

Fig Time Evolution of Outer-Layer Oxide Phase Fractions on SS-304 under Hot-Leg Conditions

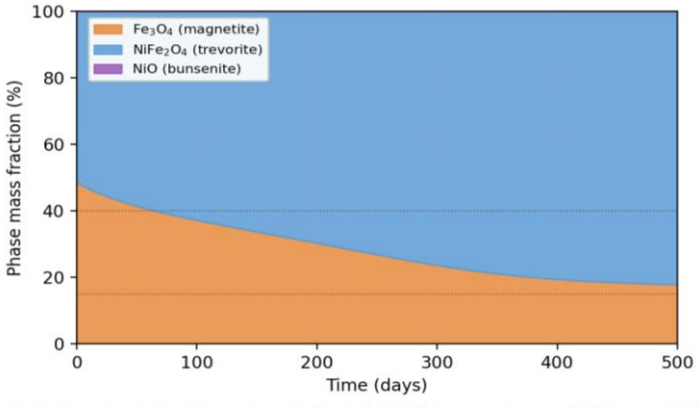

Fig Time Evolution of Outer-Layer Oxide Phase Fractions on Alloy 690 at the Steam-Generator Inlet

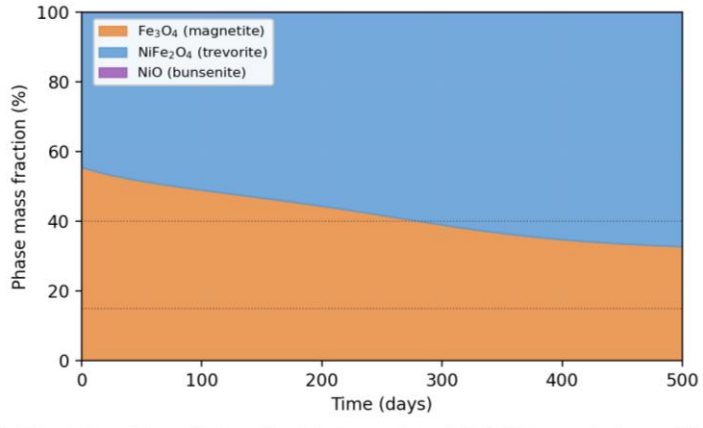

Fig Time Evolution of Outer-Layer Oxide Phase Fractions on Alloy 690 at the Steam-Generator Outlet

SNUCRUST: Results

- **[Particulate formation & outer oxide layer growth stage]**
  - S = C / C_{sat} sets dissolution–precipitation direction at each node.
  - Fe (Fe_3O_4): PWR range above V-shape minimum $\rightarrow C_{sat,Fe}$ ↑ with T
    - Cold leg: S_{Fe} ≈ 1.3 (supersaturated).
    - Hot leg / SG: S_{Fe} ≈ 0.47 (undersaturated).
  - Ni ($NiFe_2O_4$): retrograde $\rightarrow C_{sat,Ni}$ ↓ with T
    - Cold leg: S_{Ni} ≈ 0.66.
    - Hot leg / SG: S_{Ni} ≈ 0.97–0.99 (near saturation).
  - Opposite T-dependence → Fe near saturation in cold leg, Ni in hot leg.

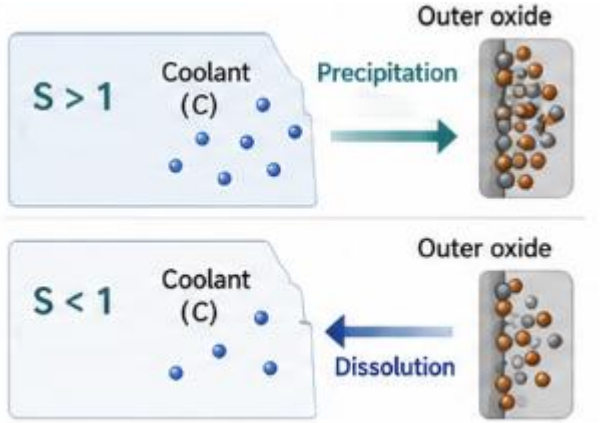

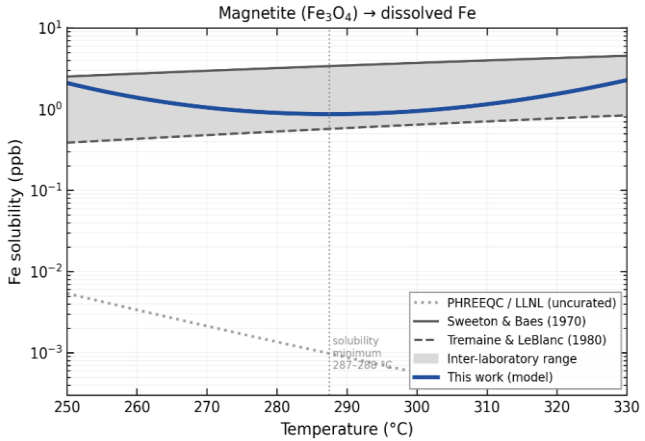

Fig Magnetite Solubility Benchmark against Literature Data

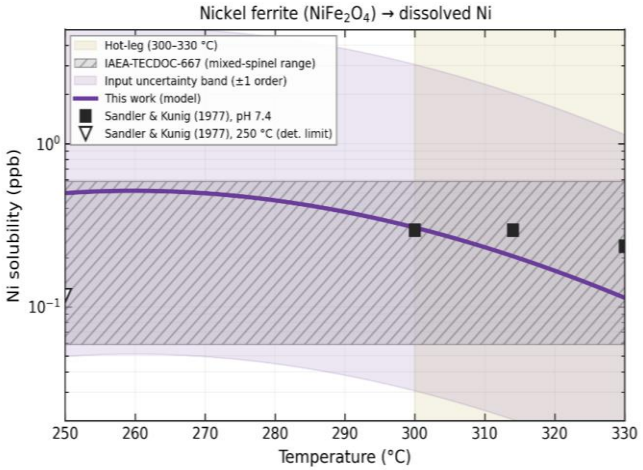

Fig $NiFe_2O_4$ Solubility Benchmark against Literature Constraints

SNUCRUST: Results

- **[Particulate formation & outer oxide layer growth stage]**
  - Only nodes with S_i > 1 contribute to precipitation.
  - 500-day budget
    - Erosion: ~1.28 mol (dominant).
    - Precipitation: ~0.90 mol (supersaturated nodes)
    - Homogeneous nucleation: ≈ 0
  - Why nucleation ≈ 0:
    - S_{max} ≈ 1.3 << CNT threshold (S ≳ 5–10)

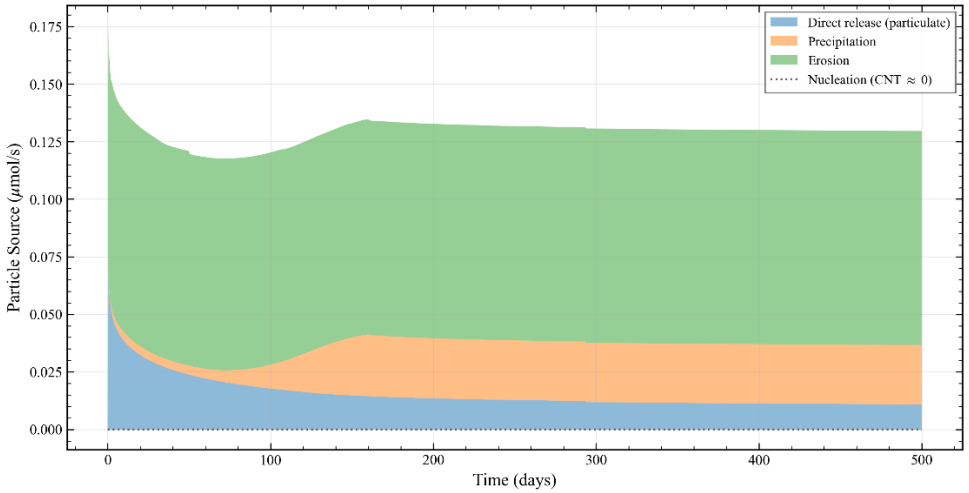

Fig Time evolution of sources of particulate corrosion products in the PWR primary coolant system

SNUCRUST: Results

- **Dissolved Fe & Ni concentration**
  - Dissolved Fe rises to ~3.00 ppb at early BOC, then decreases
    - Polley & Pick plant range 0.8–2.7 ppb — consistent
  - Dissolved Ni decreases from 0.258 ppb to 0.158 ppb
    - Polley & Pick Plant range 0.03–0.4 ppb — consistent

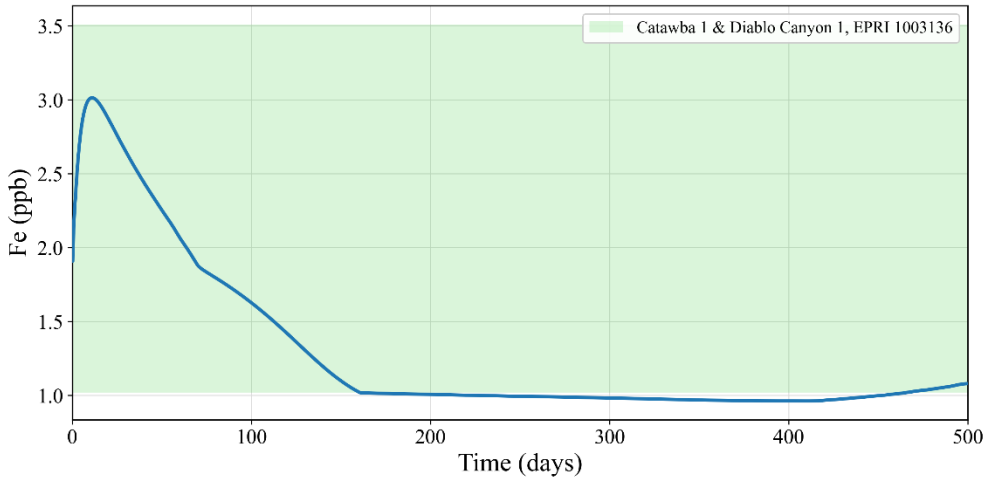

Fig Variation of Dissolved Fe Concentration over Operating Time

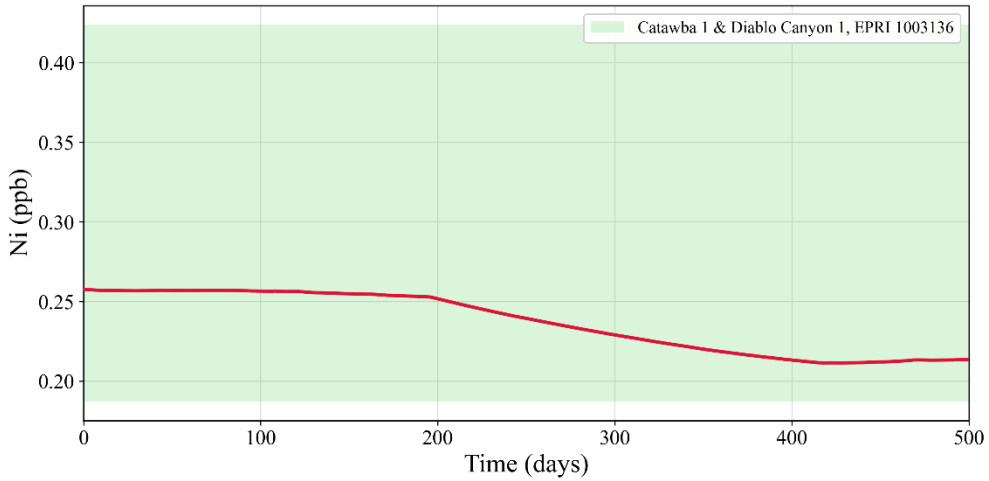

Fig Variation of Dissolved Ni Concentration over Operating Time

SNUCRUST: Results

- **Particulate Fe & Ni concentration**
  - Particulate Fe:
    - SG: 0.30–0.45 ppb.
    - CL/HL: 0.10–0.12 ppb.
  - Particulate Ni:
    - SG: 0.04–0.22 ppb.
    - CL/HL: 0.04–0.05 ppb.
  - Consistent with Catawba 1 and Diablo Canyon 1 plant data (Fe: 0.038–0.514 ppb; Ni: 0.04–0.22 ppb)
  - SG ratio $C_{Ni,SG}\ /C_{Ni,(CL,HL)}$>$C_{Fe,SG}/C_{Fe,(CL,HL)}$: large SG area + nickel-ferrite outer-layer erosion

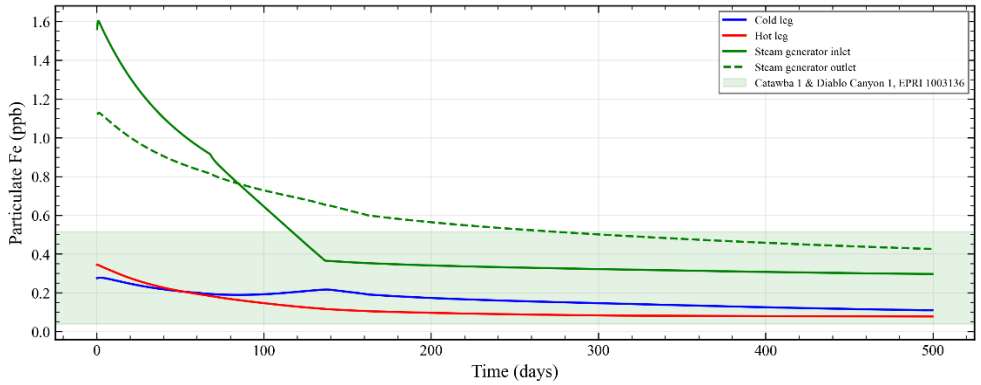

Fig Variation of Particulate Fe Concentration over Operating Time

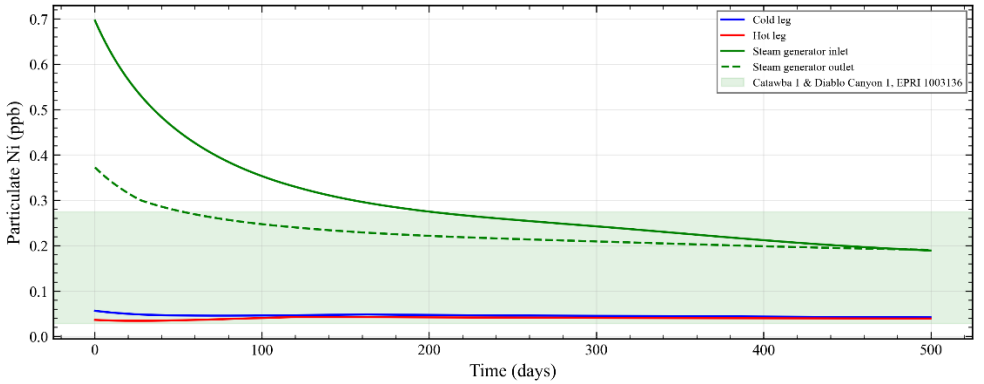

Fig Variation of Particulate Ni Concentration over Operating Time

Conclusion

1 Purpose

- Developed a PWR primary-circuit corrosion-product behavior model
- Integrated oxide growth, release, dissolution–precipitation, nucleation, erosion, redeposition, and CVCS purification
- Theory-based corrosion-product life-cycle analysis

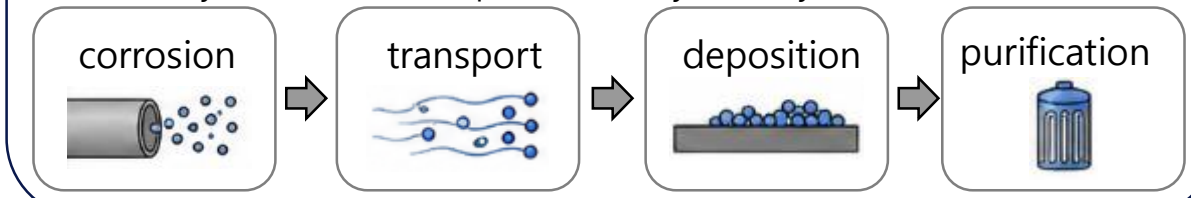

2 Solubility surrogate model

- Thermodynamic dataset for PWR primary water
- 5-D solubility surrogate
- Delivers a consistent solubility input to source-term

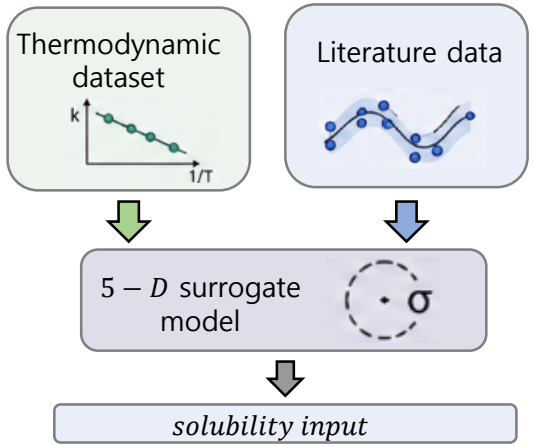

3 Differentiation from existing models

- Improves over empirical-coefficient-based models
- Allows mechanism-wise separation of contributions
- Better applicability to new alloys and operating conditions

4 Limitations & future work

Limitation

- Long-cycle accumulation and transient behavior need extension

Future work

- Coupling with the CRUD growth model for accurate growth and boron-hideout prediction
- Add a Co-58/60 activation module for radiation-source prediction
- Apply to Zn injection, SMR water chemistry, and long-cycle operation

Future Work

- **Planned extension**
  - Coupling SNUCRUST–SNUBIC
  - Add radiation source calculation from activated corrosion products and CRUD inventory.
  - Predict time-dependent source strength and spatial distribution.

Planned extension :Model Coupling

SNUCRUST

Corrosion product transport / CRUD source-term

SNUBIC

Boron hideout / CRUD growth

Planned extension :Transient operation

- Operating history
- Startup / shutdown events
- Transient driver

Planned extension :Radiation source

- Inventory / composition
- Radiation source model
- Prediction outputs

Key outputs

- CRUD / Corrosion outputs
- Transient Response outputs
- Radiation source outputs

Thank You

Dongmin Kim [professor14@snu.ac.kr]
Nuclear Fuel Cycle & Non-proliferation Lab [www.snunfc.com]

Seoul National University